Summer 7-13-2017

Examination of color center formation in CaF2 crystals when exposed to gamma and mixed neutron/gamma fields

Sara M. Pelka
University of New Mexico

Sara Pelka

Candidate

Nuclear Engineering

Department

This thesis is approved, and it is acceptable in quality and form for publication:

Approved by the Thesis Committee:

Dr. Adam Hecht, Chairperson

Dr. Gary Cooper

Dr. Cassiano De Oliveira

EXAMINATION OF COLOR CENTER FORMATION IN CAF$_2$ CRYSTALS WHEN EXPOSED TO GAMMA AND MIXED NEUTRON/GAMMA FIELDS

BY

SARA PELKA

B.S., Physics, Rutgers University, 2014

Submitted in Partial Fulfillment of

the Requirements for the Degree of

Master of Science

Nuclear Engineering

The University of New Mexico

Albuquerque, New Mexico

July, 2017

ACKNOWLEDGMENTS

Examination of color center formation in CaF_2 crystals when exposed to gamma and

mixed neutron/gamma fields

By

Sara Pelka

B.S., Physics, Rutgers University, 2014

M.S., Nuclear Engineering, University of New Mexico, 2017

ABSTRACT

Color centers in CaF_2 were studied in this work, in parallel with examinations of changes in the refractive index of the crystals by the larger research group, after they were subjected to radiation. Color centers induced by gamma rays and in mixed neutron-gamma fields were studied in CaF_2 and LiF using transmittance and absorbance spectra. The goals were to examine both neutron and neutron-gamma mixed field irradiations to be able to isolate neutron only effects and to correlate these color center effects with refractive index effects studied by our larger collaboration. Irradiation sources include ^{137}Cs, DD and DT reactions at Sandia National Laboratory, the University of New Mexico Neutron Howitzer, and the Oregon State University TRIGA reactor. Only the samples irradiated to high doses, 2.176×10^5 Gy through 2.176×10^7 Gy, at Oregon State University showed strong color centers. Different color centers had different intensities and the absorbance as a function of dose shows a clear relation and is dependent on the specific color centers. UV bleaching shows a similar relation in reverse.

Table of Contents

LIST OF FIGURES

LIST OF TABLES

Chapter 1
Introduction

Motivation

Color centers may be formed under irradiation. Gamma rays can transfer their energy to electrons, leading to electron displacements and hole creations. If those electrons or holes get trapped then there is a long-lived change in the electron/hole structure, changing the absorption properties of the material, called a color center. It is understood that the electrons and holes have a lower probability of being trapped in perfect crystals but may be trapped in locations with impurities or crystal defects.

Neutron radiation can also cause color center effects. Neutrons can cause atom displacements when they are incident onto a medium. The recoiling atoms can ionize the material, liberating electrons and holes, which then can be trapped elsewhere in the material causing color centers. These atom displacements themselves can also cause vacancies and interstitials and other point defects, which can serve as trap locations and contribute to the creation of color centers.

Radiation can produce damage and effects throughout materials which can then change their physical and optical properties, such as ductility or index of refraction for transparent media. Neutron irradiation can displace atoms, changing the density of a material which in turn changes the refractive index, which is the focus of the study by our group, but outside the scope of this thesis. By analyzing color centers, one can make an independent measurement of the radiation effects and correlate color centers effects and

the change in refractive index. Both could serve as independent modes of understanding the dose received.

Color centers are of more general interest than just in studies of radiation, particularly in CaF_2. We are interested in calcium fluoride because it is used for environmental radiation dosimetry. It also has potential applications in optics, microelectronics, and sensors [1] [2]. High purity CaF_2 crystals can also act as a window material in inertial fusion energy experiments, and they can be used in deep UV lithography and in achromatic lens systems for photography and TV lenses [3] [4]. Thus, it is important to understand and have the capability to predict whether the crystal will change colors or its index of refraction, as this might have important repercussions. The study of color centers could also be helpful in the field of electron beam lithography of CaF_2 insulating layers in microelectronics, since the larger aggregate formation is essential as input for the statistical simulation of the kinetics of metallic colloid formation and growth [5].

In addition, understanding defect damage through radiation of alkaline earth fluorides, which includes CaF_2, will be helpful when studying other fluorite structured materials such as UO_2 and $SrCl_2$.

In this thesis, color centers created through irradiation are investigated in depth. In Chapter 2, we will discuss the theory of color centers, how they are created, and what type of color centers there are, along with how different type of irradiations affect color centers. Chapter 3 has an overview of the experiment, discussing the setup and the exposures. In Chapter 4 and 5 we will look at the results of the experiment and perform analysis of the data. Additional work performed in service of the larger collaboration is

presented briefly in Chapter 6, and conclusions and future work are presented in Chapters

7 and 8, respectively.

Chapter 2
Theory

2.1 History

Color centers have been studied since the 1940's, starting with research in alkali

halides because the crystals can be grown moderately easily, with acceptable purity and

because they color without difficulty [6] [7]. Originally, the first color centers were

observed in alkali halides when they were exposed to cathode rays [7]. Figure 1 is an

example of an alkali halide after it had been exposed to x-rays. The change in color is

clearly visible as the KCl sample went from white to purple.
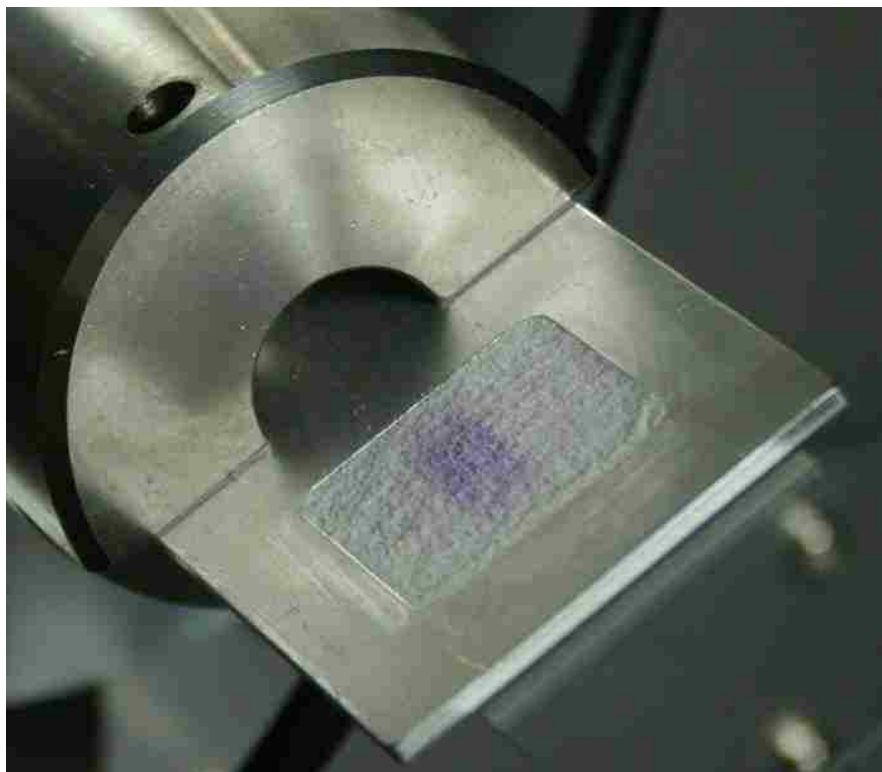
Figure 1. A sample of KCl salt after it had been irradiated with a beam of X-rays, causing
the violet color in the middle [10].

It is difficult to compare alkali halides to alkaline earth fluorides, such as CaF_2, since there is a major difference when comparing the absorption spectra between the two crystals. The difference can be attributed to a variation in the structures [8]. The first report on color centers produced in CaF_2, through x-rays, was written by Alexander Smakula in 1950, which was then followed by more thorough research done by others [9]. Most of the earlier work performed on CaF_2 focused on color centers induced through x-rays and gamma rays, or additive coloration, largely ignoring the neutron produced color centers [3].

In their original, unirradiated form, the crystals are transparent, but once they are hit with neutrons, gamma rays, x-rays, high energy electrons, or alkali-metal vapors, charge separation and ionic displacement take effect. While the band gap of the perfect material is large enough that the material appears clear, with traps there may be some energy levels within the range of the band gap. With electrons or holes moved to these traps, the material now exhibits specific coloration which can be measured using spectrophotometers [11] [6]. The coloring produced, in general, reaches a saturation point which depends on the temperature, the nature of the material, and the strength of the irradiating beam [7].

At the University of New Mexico, previous work by our group was briefly done on color centers in CaF_2 using ^{137}Cs gamma rays, but no color centers were seen. More recent work done on CaF_2 by our group is for a larger project examining radiation damage in CaF_2, which includes examining changes to the index of refraction of the crystal from neutron irradiation. The current work on color centers is performed as part of that project.

2.2 Electronic Structure

The chemical bond in an alkaline earth fluoride crystal is thought to mainly consist of ionic bonding with some amount of covalency. The structure of calcium fluoride can be thought of as a three partially overlapping face-centered-cubic lattices having the same lattice constant, with one structure composed of Ca atoms [12].

The CaF_2 crystal structure is a fluorite type structure, where the calcium atom is surrounded by eight equivalent nearest-neighbor fluorine ions [6]. In alkali halides and alkaline earth fluorides, radiation has been shown to primarily damage the halogen and fluoride sublattice, leaving the alkali sublattice intact [13].

The total width of the CaF_2 band gap has been measured to be around 12.1 eV [3] [6] [14] [15]. Because of the wide gap between the two bands, useful optical measurements of perfect crystals with fluorite structures is constrained [6]. The optical spectrum of fluorite structures is unremarkable, causing difficulties in making any conclusions regarding the material. Imperfect crystals are more interesting optically. For example, theoretical calculations have been done to calculate the energy levels of an electron localized around an anion vacancy, and they have been found to be between 3.19 eV and 3.8 eV, in the range of visible light and consistent with color center theory [8].
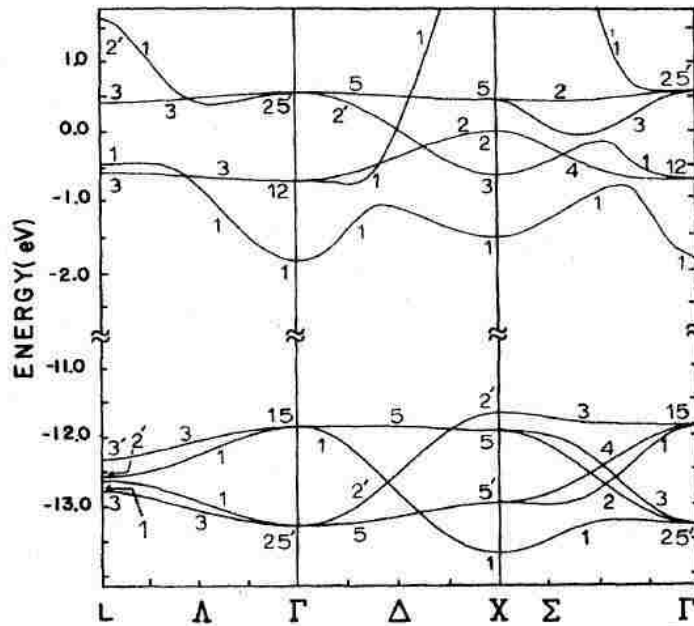
Figure 2. Valence and conduction bands of CaF$_2$ [9]

2.3 Gamma Radiation

Energy from radiation may cause electrons and holes to move to traps, thus populating color center sites. The method of energy absorption is important [11]. Since we focused on gamma irradiation and neutron irradiation, those energy transfers will be discussed in detail.

When photons impact onto the crystal structure they can interact in several ways with the electronic structure. The photoelectric effect is particularly effective when dealing with a high Z material and lower gamma-ray energies, and most of the energy of the photon is transferred to electron kinetic energy. Pair production is dominant when dealing with energies well above 1.022 MeV when an electron-positron pair is produced but this is outside the energy range of interest for this work.

Of most interest to us is Compton scattering, which dominates for photon energies above approximately 100 keV and below a few MeV. Compton scattering also depends on the Z of the material [11]. The photon transfers some of its kinetic energy to the electron kinetic energy while some of the remaining energy goes to a scattered photon. The fraction of the energy transferred to the electron in an interaction is well characterized and presented in tables. Figure 3 shows the mass attenuation (the probability of interaction) and mass energy absorption coefficient (the probability of interaction times the energy absorption fraction) of CaF_2 as a function of energy.
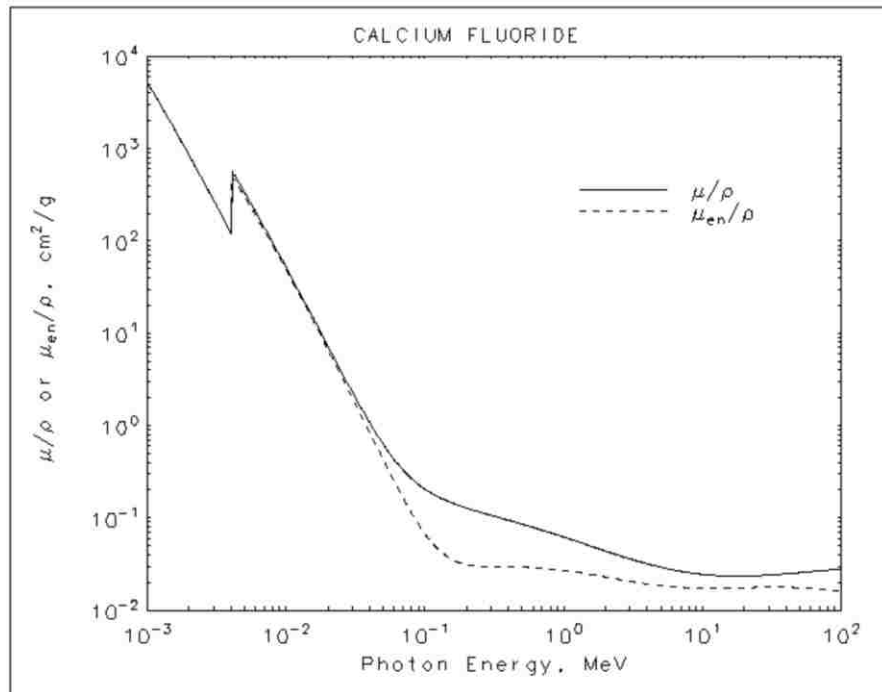
Figure 3. Mass attenuation coefficient and mass energy absorption coefficient for calcium fluoride [16].

As we are also dealing with neutron interactions in which atoms recoil, we should also understand any contribution of atom displacements from gamma rays. Figure 4 shows the photonuclear cross-section of Ca-40 as given by the International Atomic

8

Energy Agency (IAEA). It shows photon interactions at our energy of interest, around 1 MeV, are negligible because their cross-sections are close to zero. For F-19 the graphs were not available from this reference, but based on O-16, Figure 5, one can assume the gammas will not play a role in atom displacement for the lighter component of CaF_2 either. Thus, it is clear photons will interact with the electrons in the crystal, but negligibly with the atoms themselves.
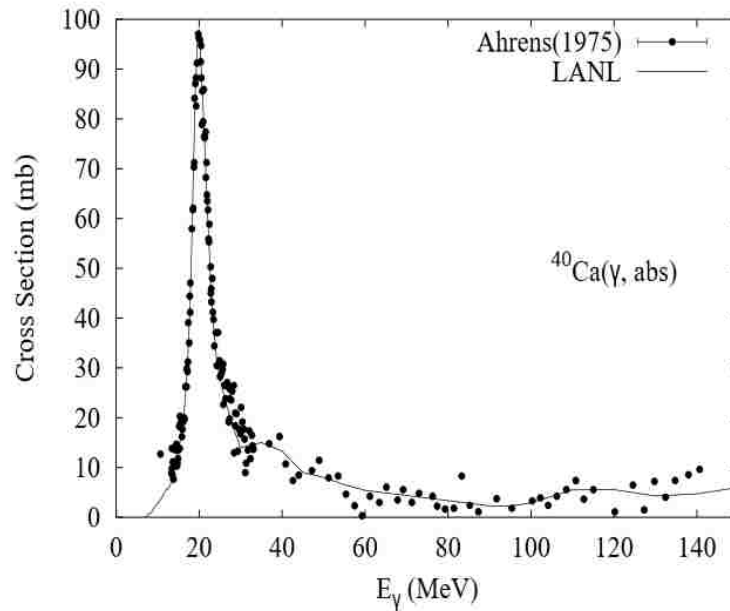
Figure 4. Photonuclear cross-section of Ca-40 [17].
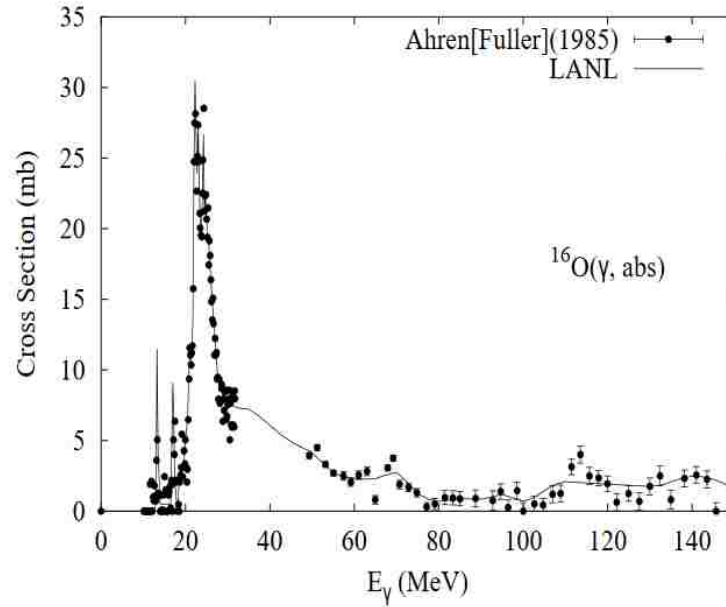
Figure 5. Photonuclear cross-section of O-16 in lieu of F-19 [17].

2.4 Neutron Radiation

Neutron radiation may both displace atoms and, through atom recoils, ionize the material and liberate electrons and holes. Thus, ionization is not purely a gamma-ray effect and it is difficult to determine the neutron only component of the damage. Neutron fields are rarely only neutrons, they tend to be mixed neutron/gamma fields. When trying to analyze the damage caused by the mixed field, the gamma ray component is subtracted from the overall response to find the neutron part [18]. In order to enhance neutron radiation effects, a radiation field with a low gamma component would be chosen.

When the neutrons hit atoms in the crystal, billiard ball collisions take place with a transfer of kinetic energy.

$$T' = \frac{4mM}{(M+m)^2} T \cos^2\theta$$

10

Here m is the particle mass, T is the kinetic energy of the particle, M is the mass of the atom, T' is the transferred kinetic energy, and θ is the angle between the incident and outgoing neutron. When there is a head-on collision, the energy transferred is maximum, so:

$$T'_{max} \leq \frac{4mM}{(M+m)^2}T$$

The energy necessary to remove an atom from its site and lodge it elsewhere is usually 3-4 times the binding energy of the solid. To achieve these high energies fast neutrons from a nuclear reactor or incident ions can be used. In comparison, electrons would have to be accelerated to close to the speed of light to produce any atom displacements [19] and so their direct contribution to atom displacement is not considered in this work.

Direct recoil atoms can displace many more atoms, also called Primary Knock on Atoms (PKA), if they have sufficient energy. The primary and secondary recoil atoms in turn moves through the lattice depositing enough energy through elastic collisions to displace other lattice ions, causing what is termed an "atom displacement cascade" [11].

2.5 Types of color centers

Color centers form when an electron or hole is trapped in a location where the lattice is not perfect. When a lattice ion or atom is missing, the lattice site is called a vacancy, and when an atom is lodged between lattice sites is called an interstitial. See Figure 6. Another possibility of a trap is an impurity, i.e., a different element than in the pure crystal.
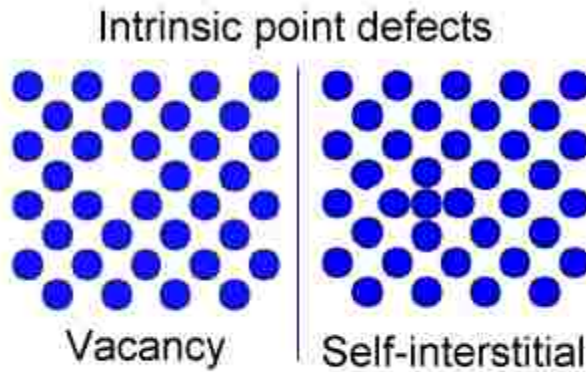
Figure 6. A graphical representation of an atom vacancy and an interstitial site [22].

Irradiation of materials causes the formation of point defects, which can absorb light in the ultraviolet to visible range [2]. The point defects involve vacancies and interstitials in combination with trapped electrons and holes, and can include impurities.

It is important to note there is a terminology difference between a color center and a color band. The color center is the point defect, whereas the color band refers to the observable changes in the absorption spectrum from many color centers being present [11]. There are several color centers that have been identified in alkali halides and alkali earth fluorides that are discussed below: F, V_k, M, and R centers.

2.5.1 F center

The F center is named after the German word "Farbe" meaning color. It is made of an electron trapped at an anion vacancy [24].

In the alkali earth fluoride structure, the energetically most favorable F center should occur at the position between two nearest neighboring fluorine sites [4] [14]. In CaF_2, the F center is composed of a single electron trapped in a fluorine vacancy, with the

nearest neighboring atoms being four cations [6]. The center has the same charge as the original anion, but it is still uncharged with respect to the rest of the lattice [11]. Figure 7 represents the structure of an F color center as seen in CaF_2. The fluorine site is vacant after being knocked out of its lattice, which will attract an electron.
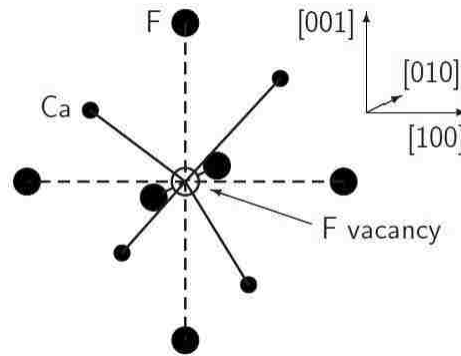
Figure 7. Structure of the F center in CaF_2. A fluorine vacancy, seen in the middle, is surrounded by four nearest-neighbor Ca atoms and six second-nearest-neighbor F atoms.

F center concentration created through neutron radiation tends to be small when the crystal is of high purity; however, using radiation has the additional advantage of being able to knock atoms out of their normal atom sites thus creating the vacancies or interstitials where electrons and holes may be trapped.

It has been noted that the F center acts like a hydrogen atom, and its point-ion potential is constant to about the nearest neighbor, at which point it rapidly increases and oscillates with increasing distance [19]. This seems to suggest the F center vacancy resembles an infinite potential well, which leads to an F-band energy in most alkali halides to be presented as

$$E_F = 17.7a^{-1.84}$$

where a is the distance in Angstroms and E_F is in eV [11].

Previous researchers theorized the F band comes from a transition between two discrete levels since the band becomes narrower at lower temperatures [7]. It was discovered the F-band absorption is the electron transition from the 1s state to the first excited state, 2p [11]. The electron might be excited to higher energy levels, which then correspond to the K and L band; however, when the F center's oscillator strength is close to unity, the F band dominates [24]. The F band in CaF_2 can be found at around 385 nm [3].

It was found that when a large number of F centers is produced in CaF_2 at 77 K, the concentration of centers diminishes when the sample is optically bleached with intense light. The residual F band however is resistant to any further optical bleaching [3]. This suggests F-aggregate centers are formed in the crystal [6].

Occasionally, the F center might acquire two electrons in the vacancy, giving it an overall charge of -1, thus the label of that defect is F^- [7] [11]. On the other hand, when the color center is missing an electron it is named F^+. This naming convention works the same for all the other types of color centers as well.

2.5.2 M center

The M center, also known as the F_2 center, is comprised of a pair of F centers residing along either the <100> or <110> direction, and made of two neighboring anion vacancies with two captured electrons [3] [26]. When an F center is irradiated, an electron is ionized, leaving an F^+ center. The electron will then be temporarily captured

by another F center to form an F⁻ center. The vacancy, which has a positive charge, is
attracted through Coulomb interactions to the F⁻ center, and the two join, creating the F_2
center [11]. Figure 9 represents the M center as found in alkali-halide crystals (top) and in
alkaline-fluoride crystals (bottom).
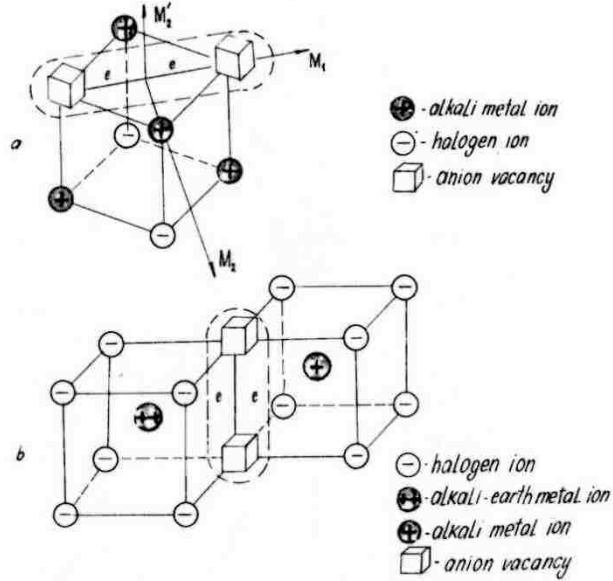
Figure 8. An example of an F_2 center, also known as an M center as seen in a) alkali-halides and b) in alkaline-earth fluorides [24].

Similar to the F center, the F_2 center is well described by a hydrogen molecule,
now placed in a dielectric medium. Long-wave optical transitions have a <110>
orientation, and are interpreted as a σ transition, which account for the major M_1 band. In
alkali halides, the energies transitions for M_1 can be calculated as

$$M_1 = 1.4d^{1.55}$$

where d is the lattice parameter [24]. There are two π transitions which are induced by
light with an intensity vector normal to the center, <110>, axis: the M_2' transition
produced by light with intensity in the <001> plane with the defect in the <110> axis, and

the M_2 transition produced by light with intensity in the <001> plane [24]. These transitions can be seen drawn in Figure 3. The luminescence bands of the M centers fall in the same emission range as for F centers' bands.

In CaF_2 it seems that the absorption band of the centers along the <100> direction dominates [6]. The M band in CaF_2 can be found around 520 nm [3].

2.5.3 R center

The R center consists of three nearest F centers, and it is sometimes referred to as the F_3 center [3] [26]. R centers follow have a <111> symmetry axis [24]. Not much is known about the R center theoretically, and most of the knowledge comes from experiments [15]. In LiF, F_3 centers luminesce around the 495 nm and 730 nm region. Generally, the R band goes down in intensity as temperature rises to room temperature [24]. The R band in CaF_2 can be found around 670 nm [3].

2.5.4 V_k center

In some ionic crystals, holes may get stuck at a specific lattice site because of powerful electron-lattice interactions; if no other lattice defects are involved, then those holes are called "self-trapped" [6]. The self-trapping is spontaneous, and it results from the localization of the hole in a covalent bond between two adjacent ions [11].

Color centers with a hole are called V centers since their absorption bands lie on the violet side of the F band. The V_k center contains a hole stabilized between two adjacent anions, which are displaced in the <110> direction [25]. Figure 9 shows an example of a V_k center in an alkali halide crystal, with a halide ion being formed in the

position of two neighboring anions, one containing a haloid atom and the other a haloid ion. The V_k band in CaF_2 can be found around 320 nm [3].
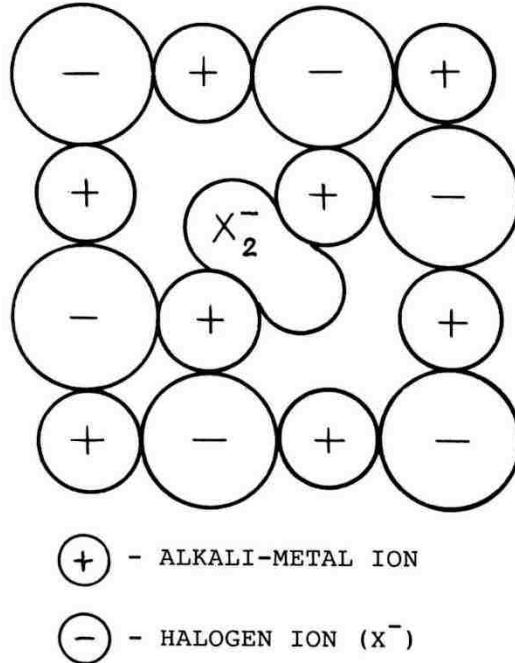
Figure 9. An example of a model of a V_k center. A molecular ion of a haloid formed on two neighboring anion positions [24].

2.6 Neutron and gamma effects with different color centers

Color centers produced through neutron irradiation are somewhat different from ones produced through x-ray or gamma-ray irradiation. An illustration of this can be seen in Figure 10, which shows a comparison between neutron and x-ray induced color centers. Comparing the two can be misleading though, since neutron irradiation can increase the temperature of the sample, such that trapped charges are removed [3]. On the other hand, ion recoils from neutrons have a high linear energy transfer (LET) and electron recoils from gammas have a low LET. Differences in the spectra may show differing populations of the different color centers caused by this ionization density. A

similar effect of differing populations is seen in scintillators from neutron vs. gamma irradiation.
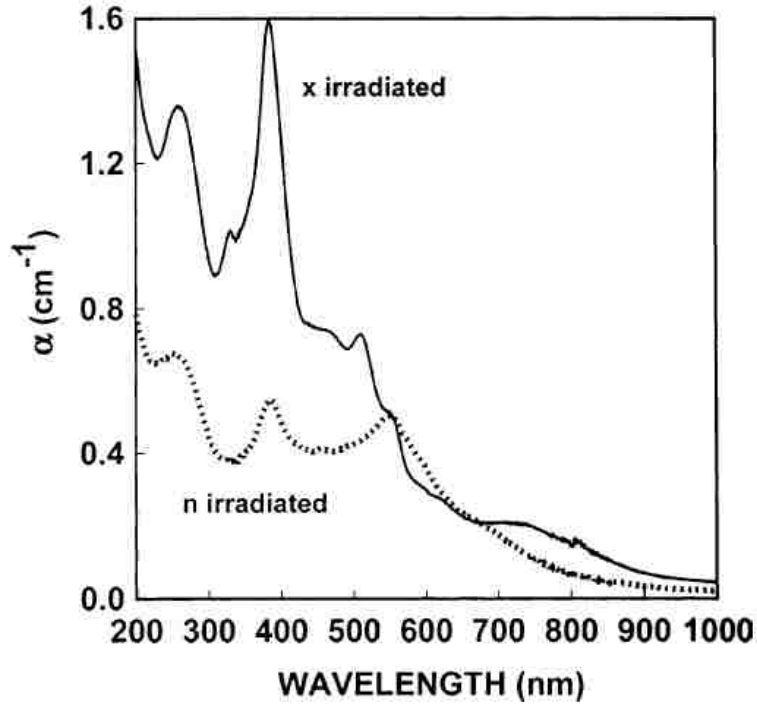
Figure 10. Comparison of color centers acquired after neutron irradiation and x irradiation [3].

2.7 Theoretical calculations

Alexander Smakula was one of the first people to study color centers in CaF$_2$ in depth and he was one of the first to analyze them and apply mathematical models to the number of color centers created [27] [28]. Theory is summarized here.

When a system is exposed to an external electromagnetic field its behavior can be described by a dielectric function ε(k,ω) whose real and imaginary parts can be related to the index of refraction and absorption coefficients of the material [19].

$$Re\ \varepsilon(\omega) = 1 + \frac{2}{\pi} \wp \int_0^\infty \frac{\Omega\ Im\ \varepsilon(\Omega)}{\Omega^2 - \omega^2} d(\Omega)$$

18

In the equation $Re\ \varepsilon(\omega)$ is related to the refractive index, and $Im\ \varepsilon(\omega)$ is related to absorption, Ω is the angular frequency variable running through the whole integration range, P is the Cauchy principal value. Both the real and imaginary parts of the dielectric constant can be obtained from experimentally found reflectivity.

Using the Born-Oppenheimer approximation [19], one gets the generalized form of oscillator strength, which can be written as

$$f = \frac{2m}{3\hbar}\omega|r(R_0)|^2$$

where r is the electric dipole and R_0 is the equilibrium position of the nuclei.

By using the generalized oscillator strength formula, we see the concentration, N, of color centers present after irradiating the crystals can be estimated from the absorption using Smakula's formula:

$$N = 0.87{\times}10^{17}\frac{n}{f(n^2 + 2)^2}W\mu$$

where f is the oscillator strength, n is the refractive index, W is the full width at half max of the band, and μ is the absorption coefficient. The absorption coefficient is defined as

$$\mu = {}^1\!/_d \ln({}^1\!/_T)$$

where d is the thickness of the sample and T is transmittance [2].

The number of color centers created from x-ray and gamma-ray radiation is directly related to the dose. Using a known beam and materials, the absorbed dose, D, can be calculated as

$$D = I\int_0^\infty \psi(E)\frac{\mu_{en}(E)}{\rho}dE$$

where $\psi(E)$ is the energy fluence per unit of energy at the point of interest, $\mu_{en}(E)/\rho$ is the mass energy absorption coefficient for photons at a certain energy, and I is a normalizing factor.

To calculate the dose received by the crystals irradiated by the Cesium-137 gamma-ray source the following equations were used.

$$\Phi = \frac{S}{4\pi r^2}$$

$$K = E * \Phi * \frac{\mu_{en}}{\rho}$$

$$D = K$$

where Φ is the flux, S is the source strength, r is the distance from the source, E is the energy of the beam, μ_{en}/ρ is the mass energy absorption coefficient of air, K is kerma, and D is dose. Kerma is equal to dose only under a specific charged particle equilibrium conditions, which allows for an approximation to the dose.

For neutron radiation, energy can be deposited by neutrons striking the atoms and causing recoils, which we discussed. The dose can be extracted from the kerma, K following

$$D = K = \Phi \, F_n,$$

where Φ is the neutron fluence for an energy interval, F_n is the kerma factor, to convert neutron fluence for the energy interval to dose in a particular material. This is summed over the range of neutron energies used. The kerma (dependent on energy transfer to

charged particles) and dose (dependent on energy absorption) are close in our energy range and allow this approximation.

2.8 Other effects

2.8.1 Temperature dependence

The optical absorption spectrum of an irradiated alkali halide crystal is dependent on temperature, which seem to also be the case for alkaline earth fluoride crystals like CaF_2, however the defects produced through irradiation in the latter crystals are less well understood than in the more commonly used alkali halides [29] [30].

Operating temperature plays a key role in the optical spectra of the calcium fluoride crystal. For instance, absorption bands appearing after low-temperature irradiation sometimes do not appear if the irradiation is performed at room temperatures [29]. Defect formation is governed by the mobility of holes. At low temperatures, defect formation is limited as the electrons and the hole do not move fast enough to be well separated, and instead recombine [13].

Research has shown that F center absorption and emission bands vary as a function of temperature, noting that as temperature increased the half-width of the band also increased, and in alkali halides the peak location shifted to lower energies [19]. When the discolored crystals were heated to higher temperatures, they started to bleach, and lose their color centers, likely because of liberating electrons and holes that were trapped which then recombine [7]. In an extreme case, when CaF_2 was irradiated at very low temperatures (77 K and 4 K), producing an F band, that F band disappeared as the crystals warmed up to room temperature [6].

Previous research has shown that single and aggregated F centers are not present at room temperature due to their mobility, low concentration of free anion vacancies and/or too high temperature where electrons are unstable [2] [31]. There is also a temperature dependence for M centers, but the band has been shown to be strong at room temperature and above [24]. Researchers measured a dependency of the lifetime of the M band on temperature, and found a temperature dependent lifetime relation

$$\frac{1}{\tau} = \frac{1}{\tau_0} + \nu * e^{-\frac{\Delta E}{kT}}$$

where $\tau_0 = 2.6s$, $\nu = 0.52$ s^{-1}, and $\Delta E = 0.006$ eV [6].

When CaF$_2$ is irradiated at room temperature, the F center is sometimes not produced or it may be converted to another type of center soon after formation [8]. In addition, the bleaching rate of point defects increases with temperature [7] [21]. An example to illustrate the temperature dependence of color centers can be found in Fig. 11 for KCl. The temperature ranges from -215 ℃ to -70 ℃ and shows a reduction in height and slight change in the centroid position of the color centers.
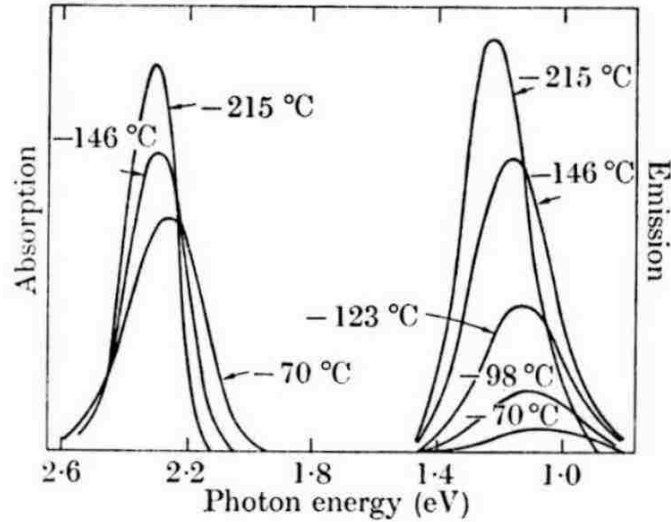
Figure 11. Absorption and emission bands for F centers in KCl at various temperatures, exhibiting the temperature dependence [32].

Temperature also has a significant effect on the electron/hole defects produced through neutron irradiation, similarly to gamma irradiation. Higher operating temperatures can cause more complex attenuation at a given wavelength, due to conversions from one defect structure to another [21].

2.8.2 Impurities

Early results of color centers in CaF_2 were inconclusive due to the crystal's sensitivity to oxygen [33]. In addition, studies of the color centers have been hindered because the absorption spectra vary greatly depending on the coloration method, crystal origin, and impurity content [34]. It has been suggested that pure CaF_2 is not responsive to radiation induced absorption, but will react when it contains impurities, such as rare earth ions [6] [26]. In fact, it was noted that the purer a crystal was, the less that color centers were produced [6]. Rare earth ions are frequently present as impurities, particularly in calcium fluoride, which can affect the absorption spectra [15]. These

23

impurities may be ionized more easily than the perfect crystal, yielding electrons that would be trapped at naturally occurring defects [3]. As an example, oxygen and hydroxyl ion impurities have a significant effect, causing the spectra to have a sharp cut-off in the far ultraviolet.

Nevertheless, literature also contradicts itself, claiming calcium fluoride can be colored through radiation and heat like alkali halide crystals, and can exhibit absorption bands in the visible and ultraviolet region [28]. Alkali halides and alkaline earth fluorides are susceptible to radiolysis, where atomic or ionic defects are formed through a series of reactions initiated by electron excitations [3]. This may be the cause of the formation of F and F-aggregate centers in LiF and CaF_2.

2.8.3 Refractive index near color centers

When irradiated, changes in the index of refraction have been noticed [20] [21]. A general change in the refractive index is related to the change in the material density, such as when atoms are displaced by neutrons. This can be described with the Lorentz-Lorentz relation [29], and is the focus of other effort by our research group.

There is also a change in the refractive index for wavelengths close to color center wavelengths which can be described by another variation of the Kramers-Kronig relation [29] presented below.

$$\Delta n(\lambda) = \frac{\lambda^2}{\pi^2} \int d\lambda' \frac{\Delta a(\lambda')}{\lambda^2 - \lambda'^2}$$

In the equation, Δn is the change in refractive index, λ is the wavelength, and Δa is the naturally induced absorption coefficient, which is wavelength dependent. Following the equation, an increase in the absorption coefficient in the visible and

ultraviolet range would result in an increase in the index of refraction. Previous research

has shown that when absorption decreases due to irradiation, the refractive index also

decreases [20].

Chapter 3
Experiment

3.1 Spectrum Analysis

To examine color centers, a Shimadzu UV-1601 spectrophotometer was used at room temperature. Figure 12 shows the spectrophotometer with the dual sample holder visible through the open door. Figure 13 shows the schematic of the optical system found inside the spectrophotometer, with the beam split going through two samples and two photodiodes on the bottom left. The spectrophotometer has two light sources: a deuterium lamp and a tungsten halogen lamp. The deuterium lamp works for the ultraviolet range, while the tungsten lamp is in the visible and near infrared range, with the light sources switching at 341.4 nm.

Figure 12. An image of the spectrophotomer used for the optical measurements.
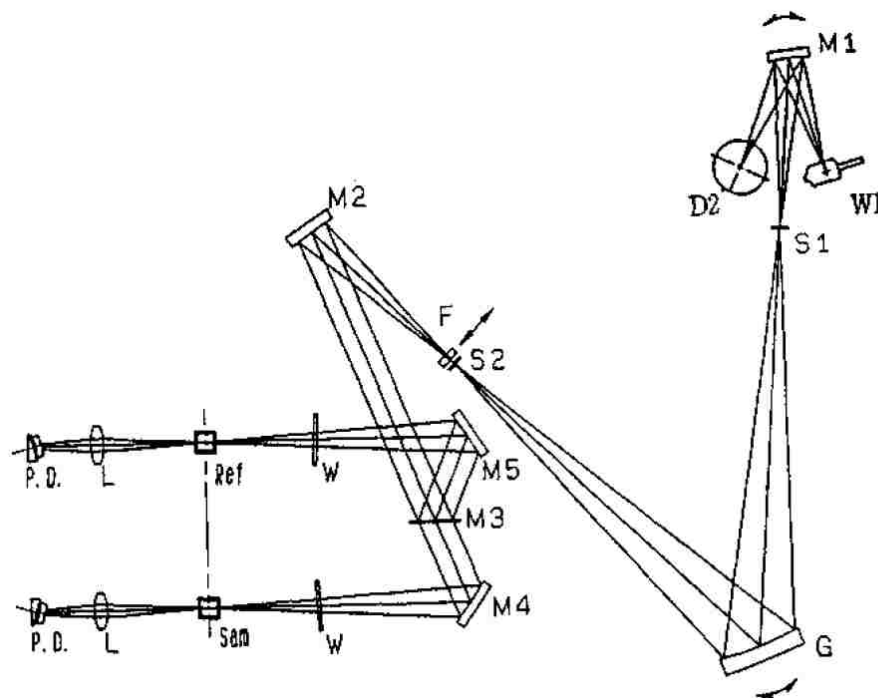
Figure 13. Schematic of the optical system inside the spectrophotometer. Explanation of symbols: M1-M5= mirrors (M3 = half-mirror), D2 = deuterium lamp, WI = halogen lamp, S1 = entrance slit, G = diffraction grating, S2 = exit slit, F = filter, W = window plate, Ref = reference cell, Sam = sample cell, L = lens, and P.D.= photodiodes [35].

To calibrate the spectrophotometer and make sure it was working properly a series of measurements were performed. Figure 14 and 15 show a calibration measurement taken of the spectrophotometer with a red bandpass filter which has a FWHM of 1.1 nm around 670.8 nm. The graphs show the machine is calibrated correctly and it is fairly accurate. Both spectra clearly show the 670.8 nm change in the spectrum. Absorbance and transmittance spectra are both presented to show the difference between the two types of measurements. The absorbance measurement, based on the log of transmittance, shows smaller details more clearly, and a second region of reduced transmittance can be seen near 850 nm.
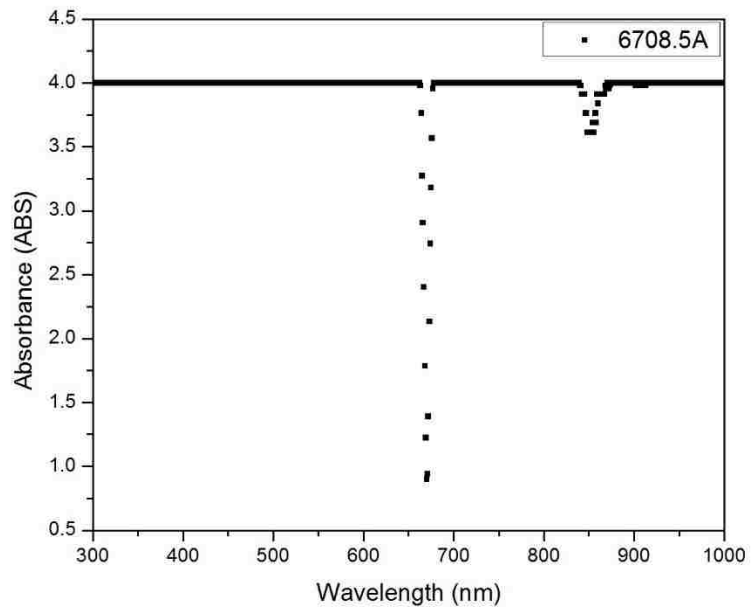
Figure 14. A graph of the absorbance of a red filter with a bandwidth of 1.1 nm around 670.85 nm to check accuracy of the SHIMADZU spectrophotometer.
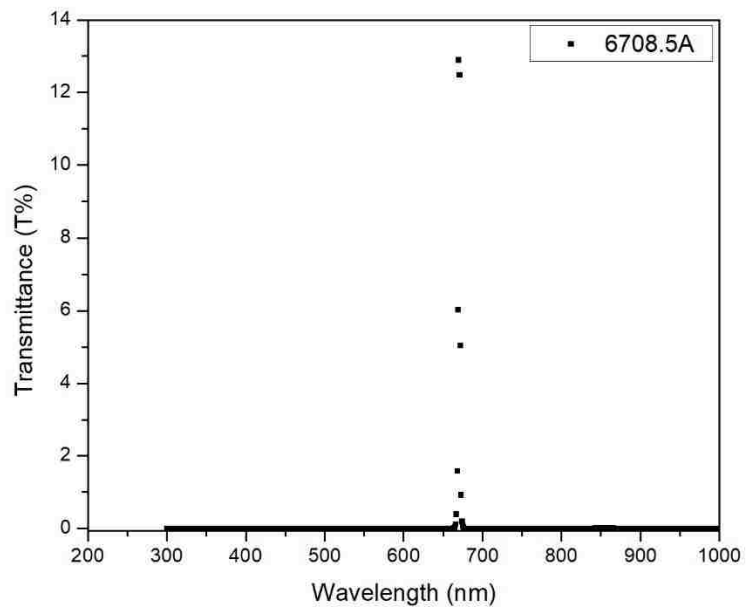
Figure 15. Graph of the transmittance spectrum of the same red filter as above to show relationship between absorbance and transmittance.

It is important to note there is a difference between absorbance and absorption: absorbance measures attenuation of transmitted radiant power while absorption measures the physical act of absorbing light. Absorbance can be related to transmittance through the following equation

$$ABS = \log_{10}(1/T)$$

where T is fraction of the original intensity transmitted through the material.

The spectrophotometer was set to transmittance and absorbance mode and raw data were accumulated. When the spectrophotometer was set to absorbance mode the spectrum ranges from 0 to 3.999, with 3.999 correlating with a minimum transmittance value of .001 or 0.01%.

To test the repeatability of the experiment and the stability of the spectrophotometer, multiple measurements were taken back to back. Figure 16 shows the results of the repeatability measurements. As one can see, the results all fall on top of each other, suggesting the spectrophotometer is stable and should produce repeatable results.
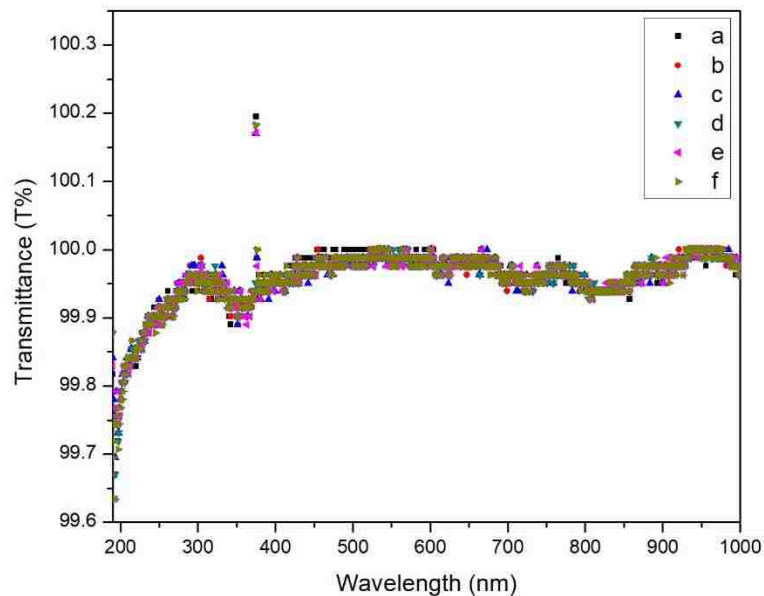
Figure 16. A spectrum of six transmittance measurements taken right back-to-back to test the stability of the spectrophotometer and the repeatability of the experiment.

3.2 Instrumentation

To take the absorbance and transmittance data the software program UVProbe 2.35 was used, in combination with the Shimadzu UV-VIS spectrophotometer. The program was used to collect both transmittance and absorbance spectra of samples.

A custom mount was made for the spectrophotometer to hold two samples at the same time to complete comparative measurements when needed. The sample holder is pictured below in Figure 17.

30

Figure 17. An image of the custom mount made for the spetrophotometer measurements.

3.3 Crystals

Several crystals were examined in this work, as there are different sensitivities for color center formation in different materials. These materials are CaF_2, $CaF_2(Mn)$, and LiF.

3.3.1 CaF_2 and $CaF_2(Mn)$

CaF_2 was chosen to complement the studies done in change in refractive index in the crystal after it was irradiated with neutrons. Since the refractive index change work is gamma blind the color center study could provide insight into radiation damage from both gammas and neutrons and, with analysis, independent neutron dosimetry. Undoped CaF_2 crystals were purchased from Rocky Mountain Instrument Company. Their dimensions were 1 inch in diameter and either 15mm or 6mm thick. For OSU TRIGA reactor irradiations, the crystals were 0.8-inch diameter with a 15mm thickness. The 1 inch diameter was chosen to fit most optic sample holders readily available, while the 0.8 inch diameter was chosen so the samples could fit inside the aluminum tubes used to irradiate samples at the Oregon State University TRIGA reactor. The thicknesses were

insignificant for this experiment, but they were vital for the study of refractive index

change measurements not included in this thesis.

Manganese doped CaF_2, $CaF_2(Mn)$, was also acquired for the experiment as these

are commonly used for optically stimulated luminescence dosimetry. The samples were

too opaque to collect meaningful transmittance or absorbance spectra, as can be seen in

Figure 18, and so they were not used.
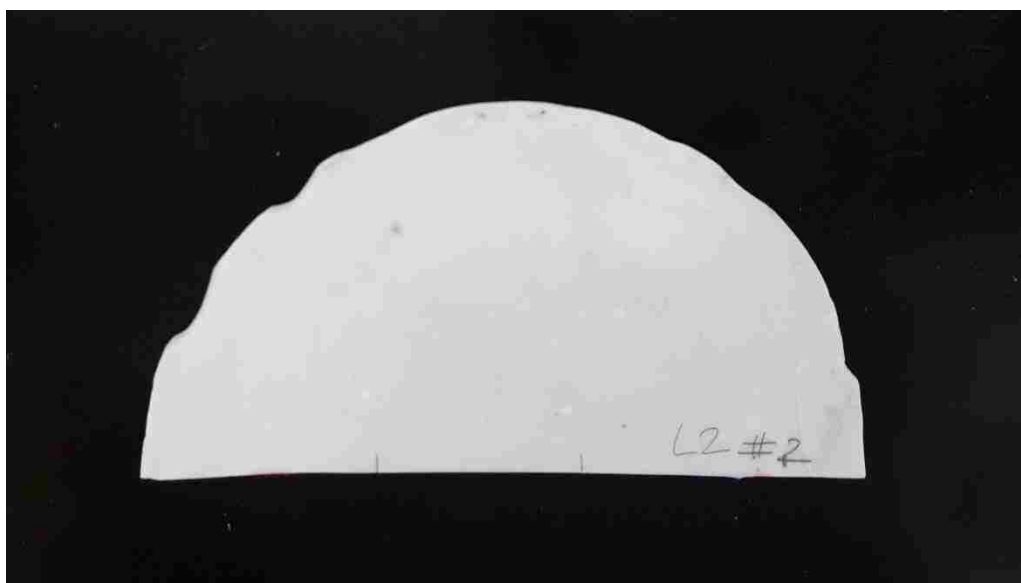
Figure 18. A picture of a sample of $CaF_2(Mn)$ set on a black tabletop. As one can see the sample is very opaque making optical measurements very difficult.

3.3.2 LiF

LiF was chosen for the experiment because it is an alkali halide, it is known to

produce color centers easily, and it has been extensively studied. Optical grade LiF

crystals were acquired from Mountain State Engineering Supplies LLC to understand the

null results we found in low dose CaF_2. The two crystals were 1 inch in diameter and 10

mm in thickness.

3.3.3 Irradiations

Neutron and gamma ray irradiations were both used. This was originally intended to examine any difference in effects and to explore subtracting out gamma ray contributions to mixed neutron-gamma fields.

3.3.3.1 Neutron Irradiation

Neutron irradiation was performed using the University of New Mexico NH-3 Neutron Howitzer, at Sandia National Laboratory, and at the Oregon State University's TRIGA reactor. Samples were irradiated for 14 days to 221 days at University of New Mexico for a neutron fluence of 4.16×10^{10}-1.31×10^{12} n/cm^2. At Sandia National Laboratory, a single crystal was irradiated with neutrons coming from DD and DT fusion reactions for a fluence of 1.85×10^{11} n/cm^2, and again for a total fluence of 2.68×10^{11} n/cm^2. Finally, crystal samples were irradiated for 0.6, 6, and 60 hours at Oregon State University for a fast neutron fluence of 1×10^{16} n/cm^2, 1×10^{17} n/cm^2, and 1×10^{18} fast n/cm^2 respectively. The doses for the OSU TRIGA reactor are far higher than from any of the other irradiations.

Two samples were kept unirradiated and used as baselines to monitor spectrophotometer performance and possible drift.

3.3.3.2 Gamma Irradiation

The CaF$_2$ crystals were exposed to gamma-rays from a 122 mCi Cs-137 source with a dose rate of 420 mR/hr at 30 cm from the source. Crystals were kept in front of the source for varying time lengths, ranging from 1 minute to about 5 days, corresponding to 7 mR and 50400 mR respectively.

The LiF crystal was exposed to the same Cs-137 source at the same distance as the CaF$_2$ samples. The crystal was irradiated for 2 hours and then for 9 days.

The same two samples were set aside to be used as baseline samples and to calibrate the spectrophotometer. Transmittance spectra were taken of the remaining eight samples before and after irradiation. The spectra were then compared to see if any changes had occurred. A second set of irradiations was performed to compare the effects over time of different samples.

Table 1 lists each crystal individually and states the crystal's dose and type of irradiation. In the second table, sample A15-5 appears twice because the sample was irradiated two separate times at Sandia National Laboratories.

The crystal irradiations were performed at room temperature for gamma radiation and neutron radiation when at the University of New Mexico and Sandia National Laboratory. The crystal temperature was higher, but still below 120 ^{o}C when irradiated in the OSU TRIGA reactor. The exact temperature was not determined.

Table 1.

Crystal identification number along with irradiation type and dose each

crystal received

Sample Number	Type of radiation, source	Dose (Gy)
A15-1	-	-
A15-2	-	-
A15-4	Neutron, UNM	1.38324-31.81455
A6-7	Neutron, UNM	0.334
A6-9	Gamma, UNM	8.986
LiF2	Gamma, UNM	8.460
A15-5	Neutron, Sandia	13.46
A15-5	Neutron, Sandia	19.84
B15-1	-	-
B15-2	-	-
B15-4	Neutron, OSU	2.176×10^4
B15-5	Neutron, OSU	2.176×10^5
B15-3	Neutron, OSU	2.176×10^6

Chapter 4
Results

Transmittance and absorbance spectra were measured for CaF_2 and LiF crystals. The manganese doped $CaF_2(Mn)$ were too opaque for the spectrophotometer and were not measured. Measurements were performed both before irradiation, to account for any impurities and to establish baselines for comparison with irradiated samples, and after irradiation. Irradiations included both neutron and gamma rays, as described before. Spectra were examined from 190 nm to 1000 nm; however, the primary focus was on the range between 300 and 1000 nm, since at shorter wavelengths the crystals already do not transmit well [2].

It was assumed that the color centers could disappear after a few days; therefore, it was necessary to take the measurements as soon as possible. This was possible with the samples irradiated at UNM, on the neutron Howitzer and the ^{137}Cs source, but it was not possible with sources irradiated externally, at Sandia and Oregon State University.

To reduce the possibility of color centers fading in room light, the samples irradiated at the Oregon State University TRIGA reactor were kept in the dark as much as possible, and kept in a dark bag and aluminum for handling and shipping. For analysis, they were taken out of their aluminum foil in a dark room, and then they were inserted into a special sample holder to do comparative measurements in the spectrophotometer. When removing from the foil and placing in the spectrophotometer, a single, dim red light was used in the room.

4.1 CaF₂ following irradiation at UNM and Sandia National Laboratory

Spectra of two CaF_2 samples were taken in the spectrophotometer using absorbance. One was measured after it had been irradiated using a Cesium source and one was the measurements of an unirradiated sample for comparison. This can be seen in Figure 19. The spectra are the same, except for the slight shift up, which may be attributed to different crystal thicknesses. No obvious color centers are visible. The only spike in the spectrum, visible at 300 nm, is also present in the unirradiated sample. This doesn't not show up in spectra from samples examined other than CaF_2, indicating it's an intrinsic property of the CaF_2 crystals we have, perhaps from impurities as this peak does not appear in published spectra of CaF_2. This can be seen in the activation analysis of the CaF2 samples irradiated in the OSU TRIGA reactor, see Appendix.
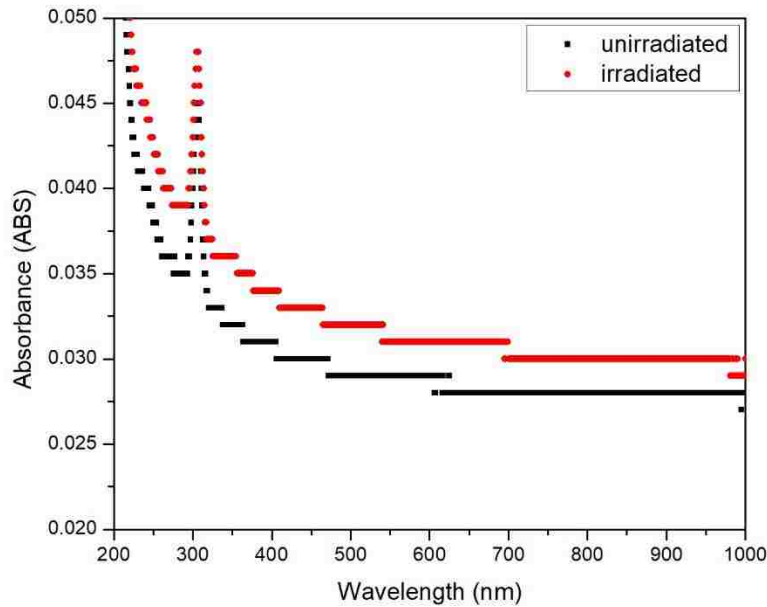
Figure 19. Absorbance spectrum of a gamma irradiated CaF_2 crystal sample, A6-9 and a standard unirradiated crystal, A6-1 in red.
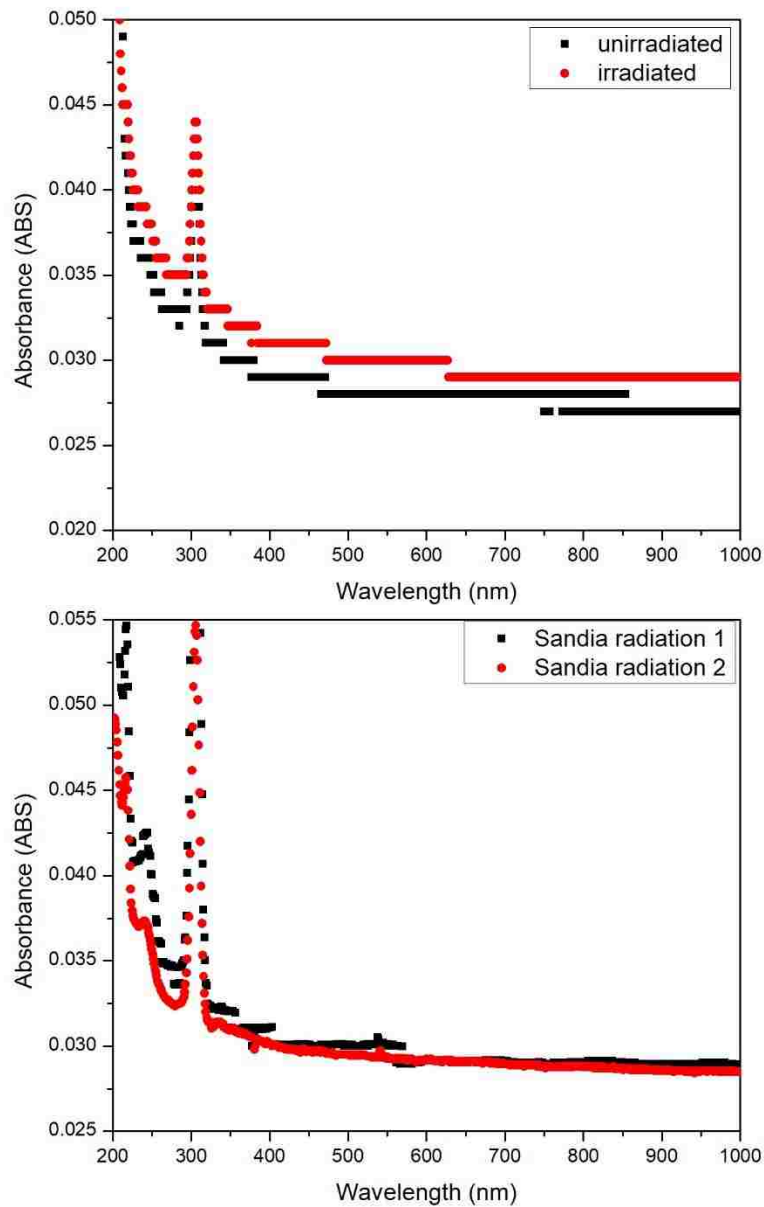
Figure 20. (top) Absorbance spectrum of a neutron irradiated CaF$_2$ sample, A6-7 in red and a standard unirradiated sample, A6-1 in black. (bottom) Absorbance spectrum of just the Sandia sample after both irradiations.

Figure 20 at the top shows the absorption spectrum of a sample irradiated in the UNM Neutron Howitzer and an unirradiated sample. At the bottom is the absorbance spectrum focusing on just the Sandia irradiated sample. There seems to be a bump around the 250 nm area, however it gets smaller with increased dose and no baselines of this crystal were taken so it is hard to say whether this is a color center. The UNM irradiated sample was placed in front of the source for 7 days, while the sample irradiated at SANDIA was irradiated with DD and DT neutrons at two different occasions for various time lengths. Like the previous plot, these graphs exhibit the same spike around 300 nm, and a vertical shift in the data, but that does not indicate a color center.

4.2 LiF following irradiation at UNM

Like the CaF_2 samples discussed in the previous section, LiF was irradiated with ^{137}Cs gamma-rays and no effects were seen. Figure 21 is of the absorption spectrum of a LiF sample after it had been irradiated with the Cesium source. It was placed as close to the opening as possible for 10 days. The spectrum is a comparison of the sample before irradiation and directly after. There are no changes in the spectrum, showing no color centers were created during the irradiation process.
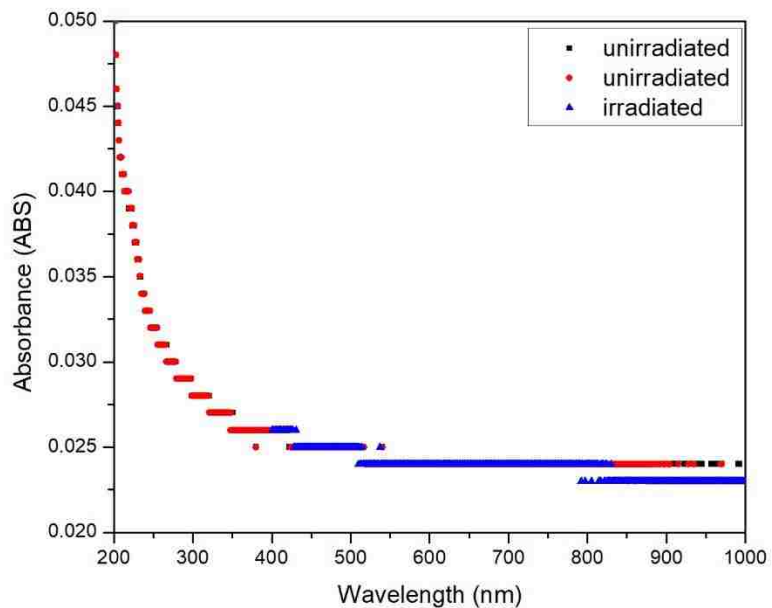
Figure 21. Absorption spectrum of a LiF crystal sample before irradiation, on 2/27/17 in black and in red, and after gamma irradiation, on 3/1/17 in blue.

LiF was also examined after it had been irradiated with neutrons inside the UNM Neutron Howitzer for 69 days. There are no changes in the spectrum, indicating there are no noticeable color centers. Figure 22 shows the graph of the same sample before and after irradiation.
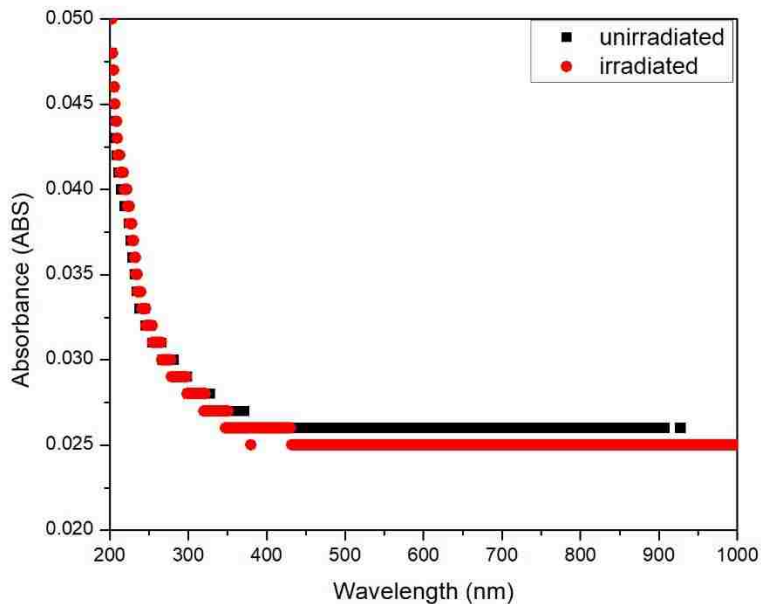
Figure 22.Absorption spectrum of a LiF crystal sample before irradiation, on 3/1/17 in black and in red, and after gamma irradiation, on 5/9/17 in blue.

4.3 TRIGA irradiations

Three samples were subjected to three different fast neutron fluences: $1x10^{16}$ n/cm^2, $1x10^{17}$ n/cm^2, and $1x10^{18}$ n/cm^2 that occurred over the course of 0.6 hours, 6 hours, and 60 hours respectively at the Oregon State University TRIGA reactor. Figure 23 shows the absorbance spectra of these three samples. The graph is significantly different from the previous ones and it features visible changes in the spectra. The $1x10^{17}$ n/cm^2 sample spectrum lets no light through between 300 nm and 350 nm, so it is impossible to deduce anything about the color bands created in that region such as proportions, only that they are strong. The same can be said about the $1x10^{18}$ n/cm^2 sample spectrum which absorbs almost everything in the visible spectrum. The most noticeable peaks are seen in sample exposed to a fluence of $1x10^{16}$ n/cm^2 where the peaks

41

are easily distinguishable. The exact gamma flux and gamma dose rate was unknown for the OSU TRIGA reactor and so doses, when given, are calculated from the neutron fluences.
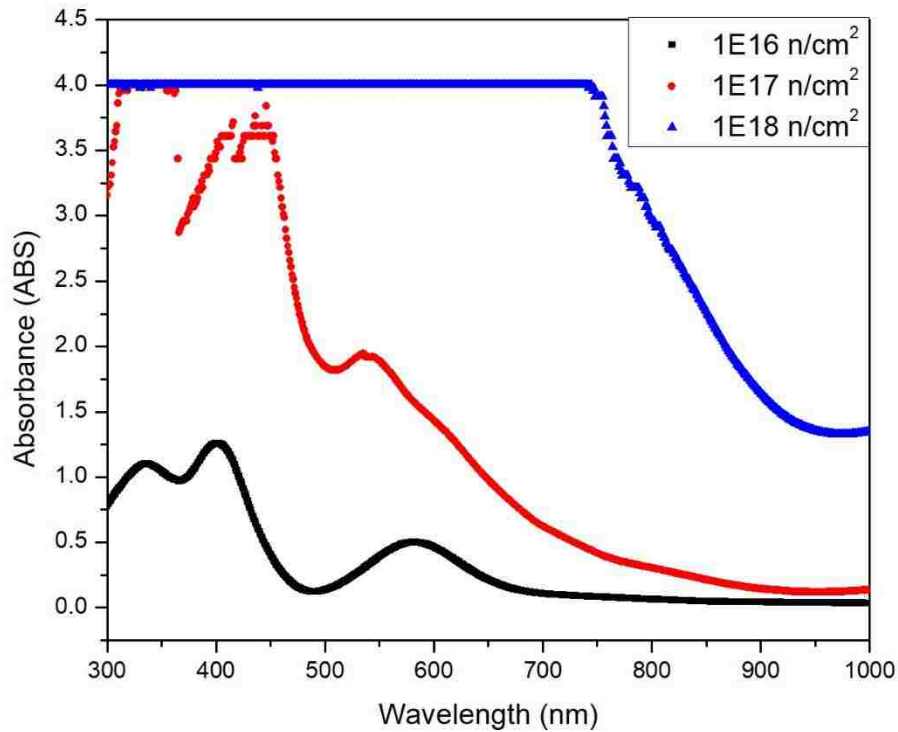
Figure 23. Absorbance spectrum of the three CaF_2 crystals after irradiation at Oregon State University. Each sample was exposed to a different fluence: $1x10^{16}$ n/cm^2 in black, $1x10^{17}$ n/cm^2 in red, and $1x10^{18}$ n/cm^2 in blue.

4.4 Bleaching

The crystals originally start off as transparent, but as they are subjected to radiation they turn a dark brown or black color. The crystal is also used for index of refraction measurements as part of the larger research project and they must transmit sufficiently at 790 nm for that project, thus bleaching of the color centers was examined. After the acquisition of the absorbance spectrum, a 7.01 W green laser was used on the CaF_2 crystals to try to bleach the color centers with intense light. Heating can also bleach

42

color centers but it was avoided to not affect the crystal structure by annealing effects.

Figures 24 and 25 show the B15-5 CaF$_2$ crystal itself after the irradiation performed at

Oregon State University. At the spot where the crystal was hit with the laser a change in

the coloration of the crystal occurred, which can be seen on the right side of Figure 25.
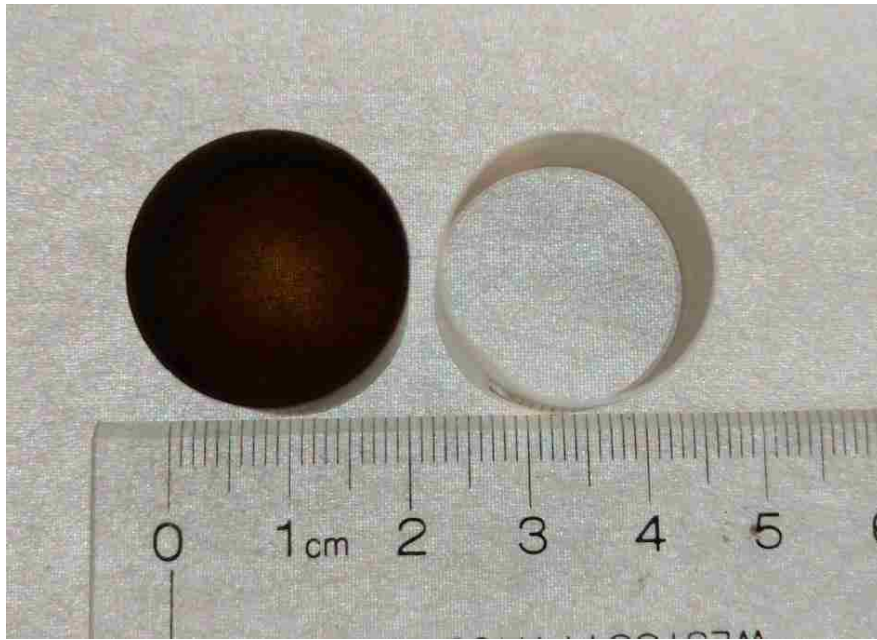
Figure 24. A comparison of CaF$_2$ crystals to show radiation damage. The left crystal has been irradiated with neutrons for a dose of 2.176x10^6 Gy and the crystal on the right has not.
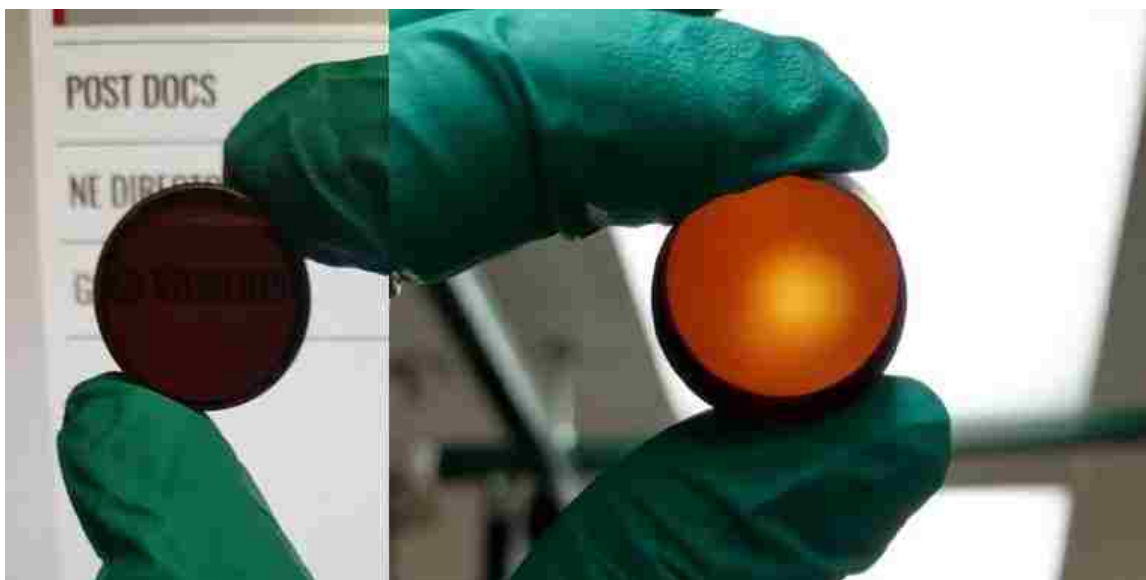
Figure 25. The same irradiated CaF$_2$ crystal before it was put in front of a laser, left side, and after, right side. The lettering on the computer screen can be seen through the crystal, but it is very dark. Bleaching occurred after the crystal was exposed to a green laser, which can be seen by the bright spot in the middle.

Figure 26-28 shows the absorption spectrum of the B15-4, B15-5, and B15-3 samples respectively after they were bleached by setting them in front of a UV lamp for several hours. Once the transmittance in the 790 nm – 795 nm range reached ~90% the samples were taken out. The absorption went down significantly, and the peaks in the 300 nm and 400 nm region are much easier to distinguish. There is also still a bump around 600 nm. In the graphs the peaks have been labeled with letters, and peak identification will be discussed later in the analysis chapter.
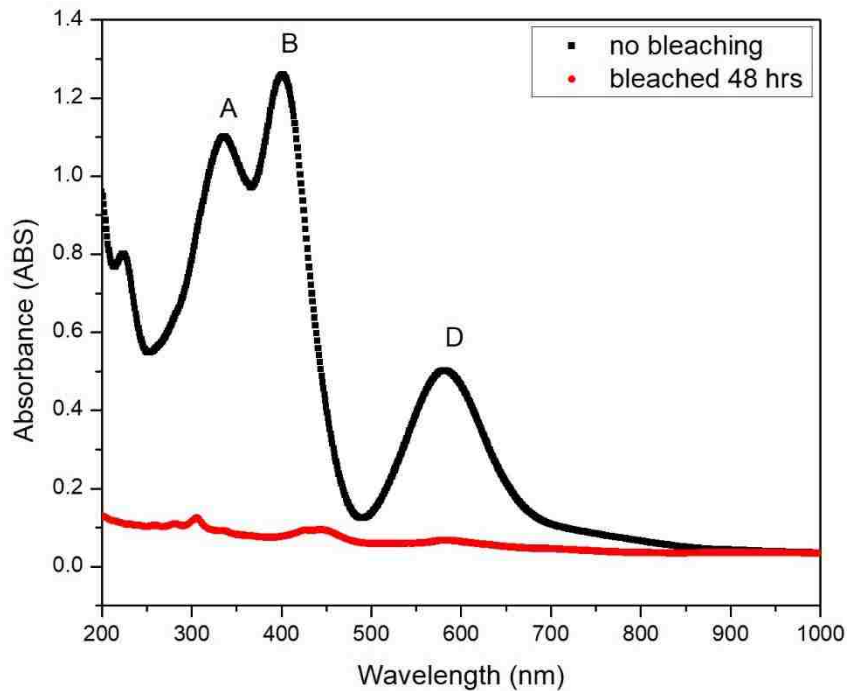
Figure 26. Spectra of the B15-4 sample immediately after it was received, and after being bleached with UV light for 2 days.
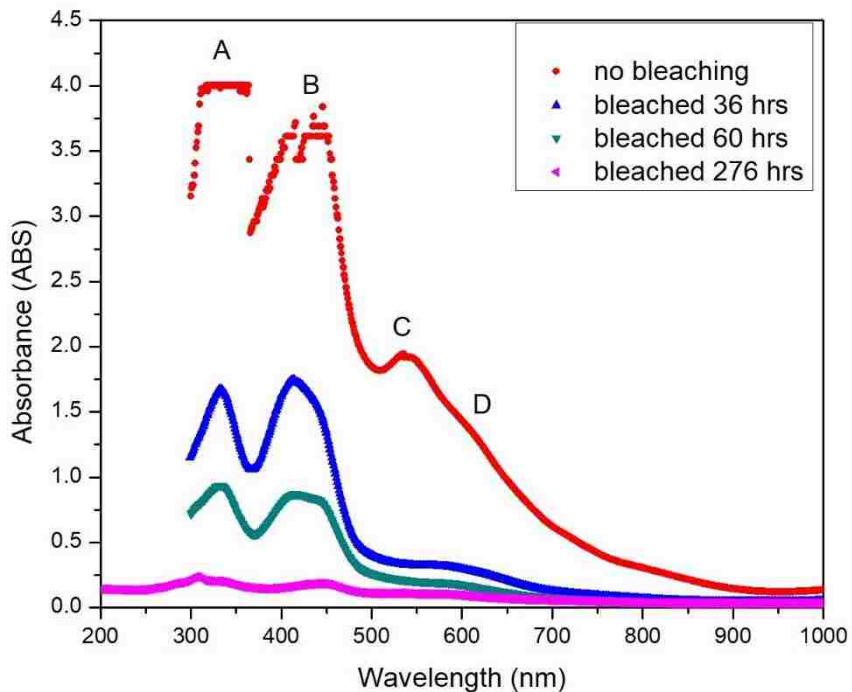
Figure 27. Spectra of the B15-5 sample immediately after it was received, and after being bleached with UV light for several days.
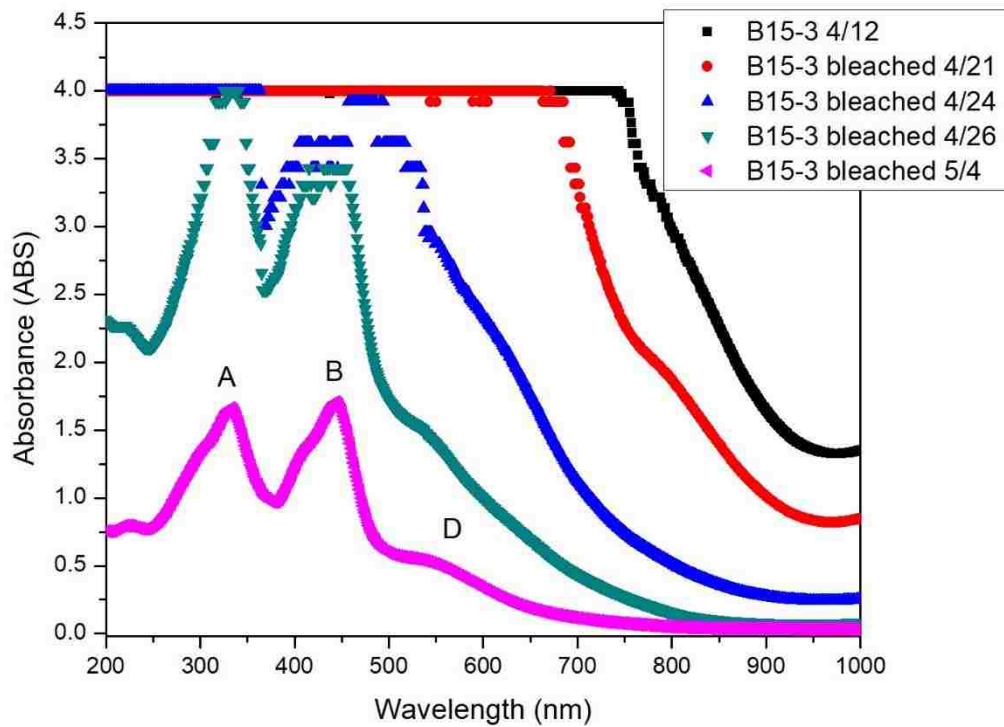
Figure 28. Spectra of the B15-3 sample immediately after it was received, and after being bleached with UV light for several days.

Chapter 5
Analysis

Previous researchers have seen color bands in CaF_2 near 255 nm, 385 nm, 455 nm, 550 nm, and 660 nm [3] [2] [28]. For LiF the color center bands were seen around 250 nm, 317 nm, 377 nm, 445 nm, 518 nm, 530 nm, 625 nm, 660 nm, 790 nm, and 950 nm [13] [2]. Unfortunately, we did not see any peaks in the spectra performed on samples irradiated at The University of New Mexico, for either type of material and type of irradiation. After consideration, the conclusion was reached that the dose those samples received was too small, though the OSU irradiated samples showed strong color bands.

To compare the samples irradiated through different fields, dose will be used. Using basic dosimetry equations, and equation X from earlier, an absorbed dose for the gamma irradiated samples can be estimated. The doses for the samples irradiated at The University of New Mexico neutron Howitzer and Oregon State University were calculated by PhD student Joe Morris using MCNP, and they were found to be 0.114 – 2.562 Gy and $2.176x10^6$-$2.176x10^7$ Gy respectively.

Figure 29 shows the graph of transmittance as a function of dose for all the CaF_2 samples used and summarizes the color center work with these crystals. The data are also presented in Table 2. Some of the samples display a transmittance of above 100%, but that might be due to noise in the data. The spectra were taken as a comparison against air, and there might have been greater transmittance through the crystal than through the air at the given wavelength. Different wavelengths were chosen to study the trends,

corresponding to different color bands that were present throughout the different crystals, and they are labeled in Figure 29 according to the labels in the Results section.
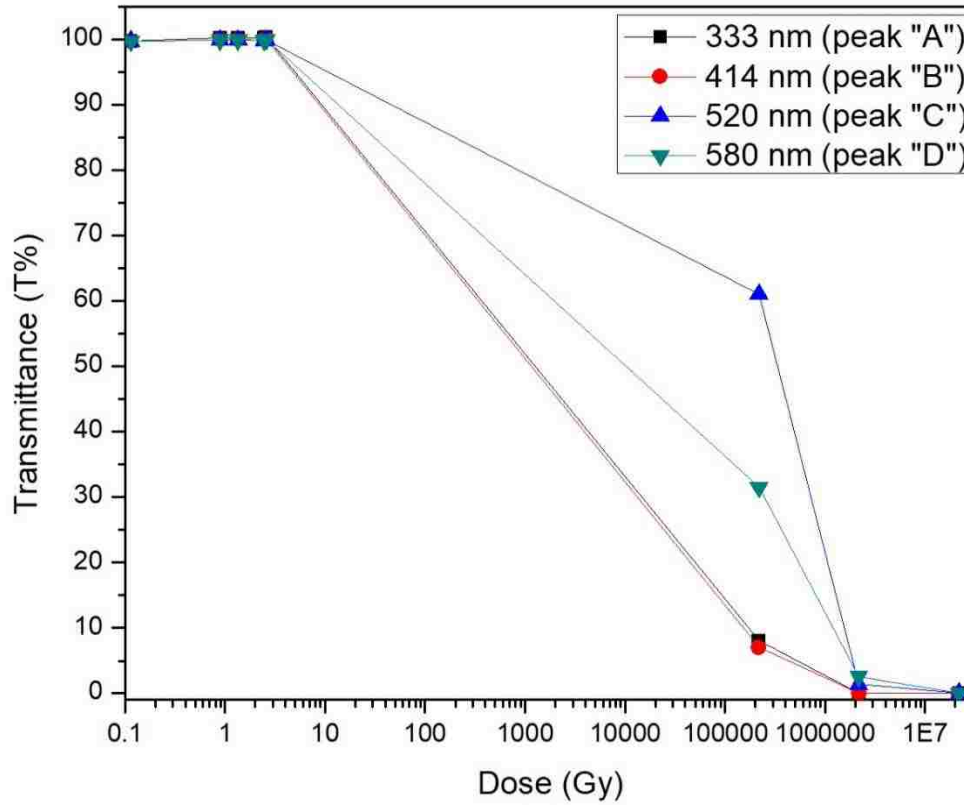
Figure 29. Graph of transmittance as a function of dose.

Table 2

The doses corresponding to the different peak heights as present in Figure 29.

Irradiation	Dose (Gy)	Transmittance (%T)			
		333 nm	414 nm	520 nm	580 nm
-	0	99.805	99.829	99.805	99.817
UNM	0.114	99.719	99.731	99.719	99.719
UNM	0.8912	100.183	99.927	99.915	99.902
UNM	1.353	100.232	100	99.927	99.939
UNM	2.451	100.195	99.939	99.829	99.878
UNM	2.562	100.342	100.037	99.89	99.951
OSU	2.176×10^5	7.996	7.043	61.06	31.519
OSU	2.176×10^6	0.01052	0.02443	1.40281	2.56448
OSU	2.176×10^7	0.01	0.01	0.01	0.01

A trend was noticed in Figure 29, where different bands responded to the UV light differently. The same wavelengths that were chosen earlier were then analyzed to determine how they change as they are subjected to UV light. Analyzing the spectra from Figure 26, Figure 30 shows the changes in band transmittance as a function of time for sample B15-4, which had absorbed a dose of 2.176×10^4 Gy with 0.6 hours in the OSU TRIGA reactor. The bands occurring at wavelengths 333 nm and 414 nm follow the same trend, and are almost identical.

Figure 30. An image of the bands present in crystal B15-4 (0.6 hours at OSU reactor) at different wavelengths and how they change after being exposed to UV light for varying times.

Analyzing the spectra from Figure 27, Figure 31 shows the changes in band transmission as a function of time for sample B15-5, which had absorbed a dose of 2.176×10^5 Gy with 6 hours in the OSU TRIGA reactor. The 333 nm and 414 nm bands once again follow a similar trend in Figure 31, as we saw earlier in Figure 30. The bands that took the larger dose to significantly reduce transmittance - 520 nm and 580 nm - appear to be the first ones to bleach under UV light.
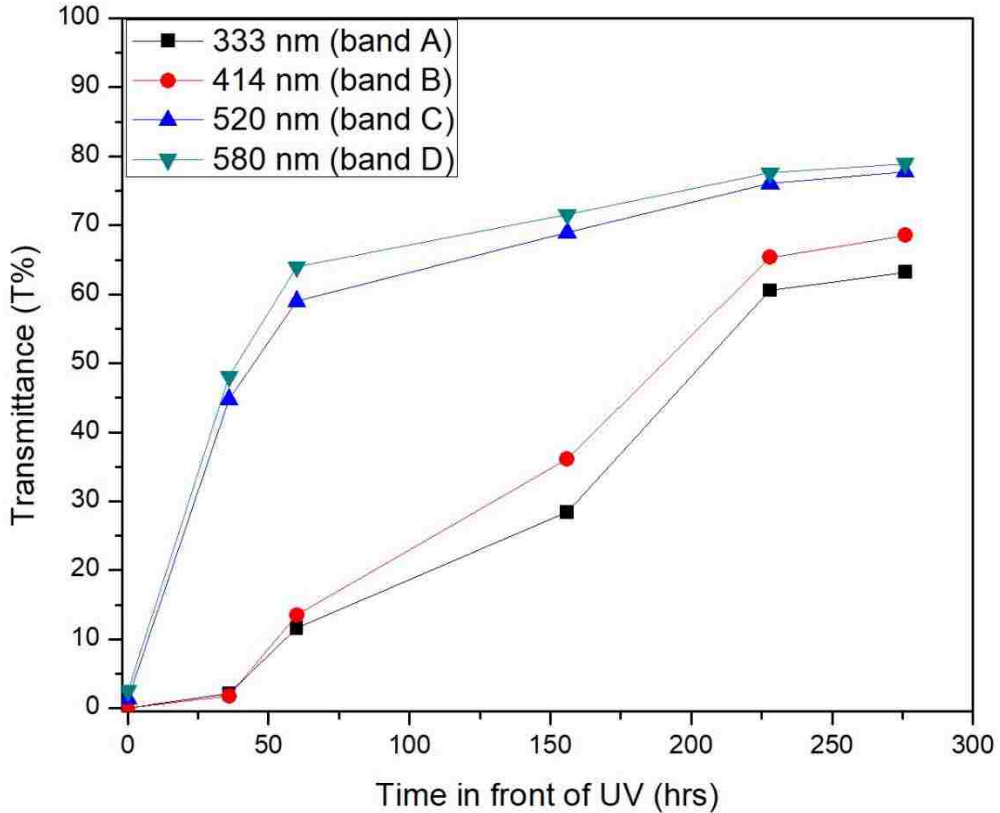
Figure 31. An image of the bands present in crystal B15-5 (6 hours at OSU reactor) at different wavelengths and how they change after being exposed to UV light for varying times.

Finally, analyzing the spectra from Figure 28, Figure 32 is the image of crystal B15-3, subjected to a fluence of $1x10^{18}$ n/cm^2 and a dose of $2.176x10^6$ Gy with 60 hours in the OSU TRIGA reactor. The effective time spent in front of the UV, in reality, is shorter because the sample was initially placed behind B15-5 until a better arrangement was introduced. That might also partially account for the slow bleaching seen at the beginning. Once the crystal starts to bleach though it seems to follow the trend seen in Figure 30, where the 333 nm and 414 nm band stick together, while the 520 nm and 580 nm bands separate and they bleach at a slower rate than the previous bands. Unlike in sample B15-4, though, where the 580 nm band is above the 520 nm band.
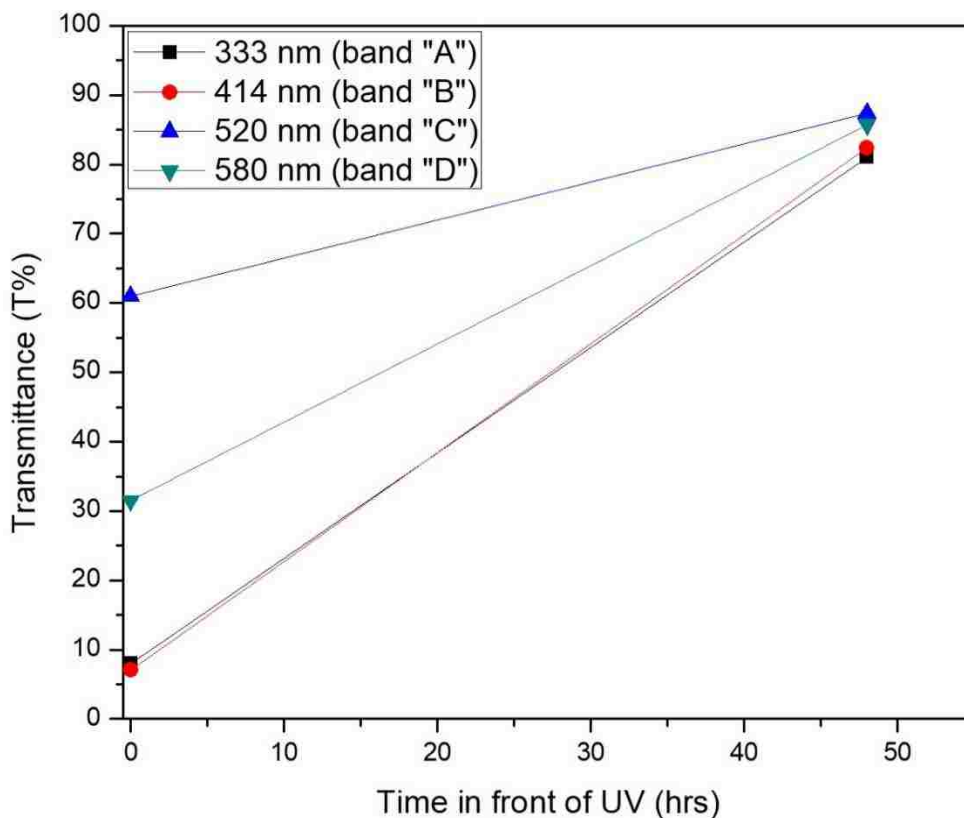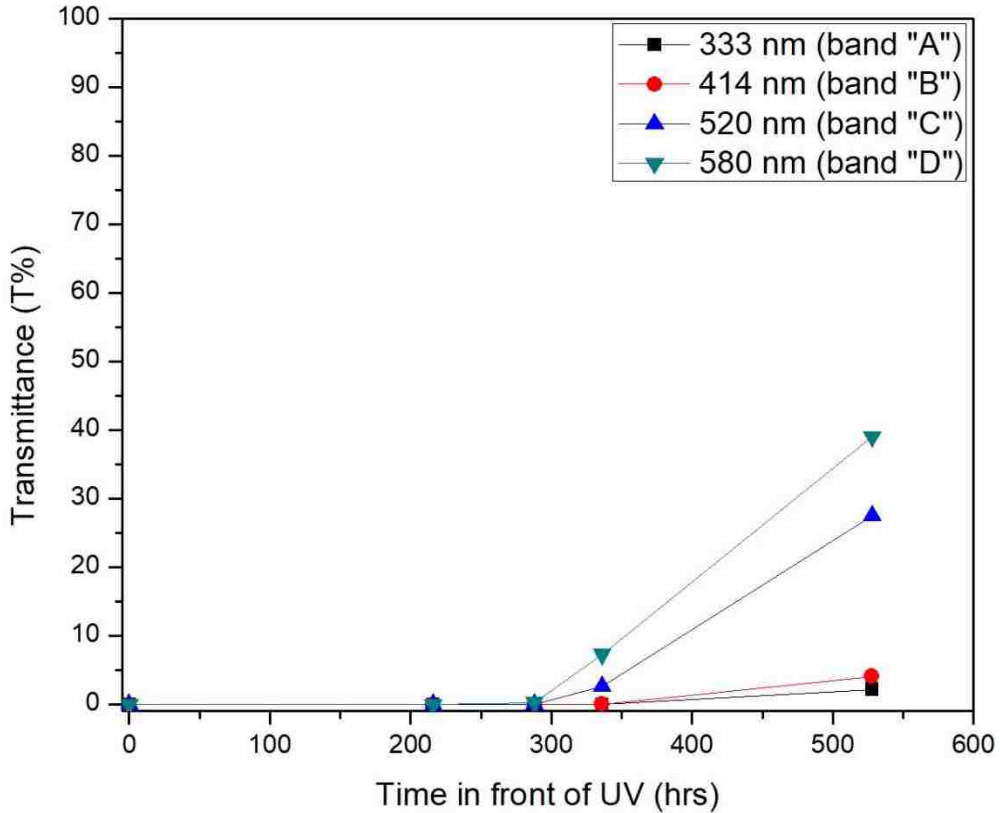
Figure 32. An image of the bands present in crystal B15-3 (60 hours at OSU reactor) at different wavelengths and how they change after being exposed to UV light for varying times.

As mentioned earlier, no color bands were apparent from our ^{137}Cs irradiations. For a source strength of 122 mCi for the ^{137}Cs source, about 10 cm to the crystals, a gamma-ray energy of 662 keV, and an irradiation period of 10 days, the calculated dose in the CaF_2 crystals was found to be 8 Gy. Compared to previous research that used neutron fluences of 1.1×10^{19} [3], this is significantly lower, which is a possible reason for why there were no color bands present in the crystals while the cited work was able to measure them.

Color centers were also not seen from our neutron Howitzer irradiations or from Sandia D-D and D-T irradiations. The doses produced were also low compared to other

researchers', ranging from 0.114 Gy to 2.562 Gy for the Neutron Howitzer, and 314.90 and 470.58 Gy for Sandia National Laboratory.

On the other hand, color centers were measured on our samples from the Oregon State University reactor. Samples B15-4, B15-5, and B15-3 from Oregon State University were irradiated for 0.6, 6, and 60 hours, respectively.

Crystal B15-4 was irradiated for 0.6 hours, with a fast neutron fluence of $1x10^{16}$ n/cm^2 and an absorbed dose of $2.176x10^5$ Gy. The peaks produced by the radiation are small, but when viewed in Figure 26 they are easier to distinguish. There are 4 peaks present, but only three fall in the visible spectrum range. The peaks seen fall in 350 nm, 400 nm, and 600 nm.

In crystal B15-5, which was irradiated for 6 hours, the total fluence of neutrons the crystal absorbed was $1x10^{17}$ n/cm^2, leading to an absorbed dose of $2.176x10^6$ Gy, as calculated by MCNP. The spectrum displays a significant rise in absorption, which can be compared to the wide peaks seen by Cooke and Bennett in Los Alamos [3]. The 550 nm peak is the easiest to spot, but the 385 nm and the 455 nm peaks merged together and thus it is hard to tell them apart. There is a slight bump on the graph around the 650 nm region, which could represent the 660 nm peak seen by others.

Sample B15-3, irradiated for 60 hours, received $1x10^{18}$ n/cm^2 fluence and $2.176x10^7$ Gy dose. The crystal came back completely colored black. The spectrum allowed < 0.01% transmittance over the whole wavelength range chosen, which did not provide any information regarding the color band locations, but showed they were strongly present.

For each of the three graphs three bands are present, and in Figures 26-28 they have been labeled A, B, and D corresponding to peaks at 333 nm, 414 nm, and 580 nm respectively. In Figure 27 there might be an additional peak, labeled C at wavelength 520 nm. Peak A corresponds the most to the V_k band, however it is strange we are seeing it, since it thermally decays above 140 K [3]. All three peaks were also seen by Alexander Smakula in 1954 when he saw a band at 335 nm, 394 nm, and 574 nm in multiple crystals [26] [36]. Alexander Smakula believes the band at 394 nm is a Mollwo β band, which is an M band [6]. This corresponds to our band labeled "B." The F band occurs at 375 nm [22] [3] therefore we probably did not see that band. Bands "C" and "D" are unknown for now, and they are probably made of a less common color centers, such as F^-, R, or N.

As seen in figures 30 - 32, different bands showed different responses to the irradiation and the bleaching. Bands at 333 nm and 414 nm responded the most to the radiation. When they are irradiated with a higher dose they also appear less affected by UV bleaching. This suggests the bands are made of color centers that need more energy to be bleached. The two bands responded very similarly to each other to both irradiation and bleaching. Only in sample B15-4 one can notice differences between the two bands: the 414 nm band populated faster and it has a higher absorbance. At the early stages of optical bleaching, as seen in all three graphs, these two bands responded almost identically, but with further bleaching, as seen in Figure 31, the 414 nm band depopulates faster than the 333 nm band.

On the other hand, bands found at 520 nm and 580 nm originally needed larger doses to reduce transmission and they were the more easily bleached. This suggests the two bands are composed of color centers with greater charge mobility. For the two

samples with the stronger color centers (B15-5 and B15-3) the 520 nm and 580 nm bands bleach similarly, with the 580 nm band having slightly more transmittance. For sample B15-4, the 520 nm band starts with higher transmittance than the 580 nm band. While both bands bleach, they don't track, starting from such different values. It is interesting to note the 520 nm band is completely missing from Figure 26, suggesting a certain dose threshold needs to be reached before the band appears but once it appears it's so close to the 580 nm band such that the two seem to join. Not enough information is available at the moment to relate this information to which color centers these bands might be composed of.

To isolate the neutron caused damage, it is important to know the gamma portion of the spectrum that produced the color centers in the Oregon State samples. Unfortunately, the exact gamma flux and gamma dose rate was unknown for the OSU TRIGA reactor and thus it is hard to determine how much coloring was caused by the neutrons themselves versus the gammas.

Chapter 6
Additional Work

Previously, work was done on study of the change in the index of refraction in a material after it has been subjected to radiation along with student J. Morris, and our collaborators in physics Prof. J.C. Diels and student J. Hendrie. As crystals are damaged by neutrons, the crystal may swell, changing the index of refraction. This is measured to high precision by a nested cavity technique, described in our previous work [36]. Due to the low atom recoil probability for the relevant gamma energies, this technique is gamma blind. Therefore, the color center measurements, which are very sensitive to gamma radiation and neutrons, provide complementary information.

In the refractive index project, I performed work on the laser setup, such as helping mount and setting up the optical equipment. In addition, help was provided in the data collection by taking the measurements of the crystals and by helping start the application of corrections to the mounts to improve data acquisition. Unfortunately, no results were acquired while still working on the project and before moving on to the examination of color centers.

Chapter 7
Conclusions

Color centers were produced in CaF_2 when subjected to high doses. All the crystals irradiated at University of New Mexico and Sandia National Laboratory were insufficiently irradiated, producing no obvious color bands and showing a clear lower limit on measurable results of above 3.515 Gy. This lead to the conclusion that in low dose environments CaF_2 crystals do not produce strong enough color bands. Irradiations at much higher doses such as 2.176×10^5 Gy to 2.176×10^7 Gy performed at the Oregon State University reactor showed color centers. Color bands were noticed in the 333 nm, 414 nm, 520 nm, and 580 nm regions, which might correspond to the V_k band, M band, and two unknown bands respectively. The color center work shows that dosimetry may also be possible using color centers, though we were not able to see color bands at lower doses and we do not have high dose data from gamma rays to compare with neutrons.

Color center production was attempted in two other materials: LiF, an alkali halide, for confirmation of our earlier seen results and $CaF_2(Mn)$ since it is used in optically stimulated luminescence dosimetry. After irradiation with both gammas and neutrons we saw no color centers in LiF, and thus no conclusions could be drawn. Manganese doped CaF_2 was too opaque to perform any optical spectra.

After examining the color centers in the CaF2 samples irradiated at the OSU TRIGA, those samples were UV bleached to make them more transparent for the index of refraction measurements. Bleaching effects progressed with UV exposure. As seen in Figures 29 and 30, different bands showed different responses to the irradiation and the

57

bleaching. Bands at 333 nm and 414 nm responded the most to the radiation while also being less affected by UV bleaching. The two bands responded very similarly, and at the early stages of optical bleaching they responded almost identically. On the other hand, bands found at 520 nm and 580 nm originally needed larger doses to reduce transmittance and they were the more easily bleached. In addition, for different samples, the bands' transmittances sometimes switched places, where sometimes the 520 nm band would be more transparent and at other times the 580 nm band would be more transparent.

Chapter 8
Future Work

For future work, the research can be tied into other work done by by our research group to help analyze radiation damage and effects. Neutron radiation can displace atoms, which can change the density of a material and thus the refractive index. Optical measurement of this refractive index change is being used to relate to neutron dose. One could try to correlate the color centers to the refractive index measurements of radiation damage, to understand semi-permanent and permanent effects that appear.

Future work should examine different crystals. Sapphire is of interest since it can produce color centers relatively easy and it would be applicable to the experiment focusing on the change in index of refraction.

Before all this future work is done, the most important next step would be to irradiate the samples between the doses available at University of New Mexico and the Oregon State University TRIGA reactor, as this appears to be where the largest color band changes happen.

References

[1] M. Chougaonkar and B. Bhatt, "Blue light stimulated luminescence in calcium fluoride, its characteristics and implications in radiation dosimetry," *Radiation Protection Dosimetry,* vol. 112, no. 2, pp. 311-321, 2004.

[2] M. Izerrouken, A. Meftah and M. Nekkab, "Color centers in neutron-irradiated $Y_3Al_5O_{12}$ CaF_2 and LiF single crystals," *Journal of Luminescence,* vol. 127, pp. 696-702, 2007.

[3] D. Cooke and B. Bennett, "Optical absorption and luminescence of 14-MeV neutron-irradiated CaF_2 single crystals," *Journal of Nuclear Materials,* vol. 321, pp. 158-164, 2003.

[4] H. Shi, L. Chang, R. Jia and R. Eglitis, "Ab Initio Calculations of the Transfer and Aggregation of F Centers in CaF_2," *The Journal of Physical Chemistry,* vol. 116, pp. 4832-4839, 2012.

[5] A. Puchina, V. Puchin, E. Kotomin and M. Reichling, "Ab initio study of the F centers in CaF_2: Calculations of the optical absorption, diffusion and binding energies," International Centre for Theoretical Physics, Trieste, 1997.

[6] W. Hayes, Crystals with the Fluorite Structure, Belfast: Oxford University Press, 1974.

[7] F. Seitz, "Color Centers in Alkali Halide Crystals," *Reviews of Modern Physics,* vol. 18, no. 3, pp. 384-408, 1946.

[8] T. Kamikawa, Y. Kazumata, A. Kikuchi and K. Ozawa, "The F center in calcium fluoride," *Physics Letters,* vol. 21, no. 2, pp. 126-128, 1966.

[9] A. Smakula, "Bleaching of CaF2 crystals colored by x-rays," *Physical Review Letters,* vol. 91, no. 6, pp. 1570-1571, 1953.

[10] "MRSEC Education Group," University of Wisconsin-Madison, 13 March 2007 [Online]. Available: http://education.mrsec.wisc.edu/background/F_center/ [Accessed 6 April 2017].

[11] F. Brown, A. Franklin, R. Fuller, B. Henderson, A. Hughes, K. M, C. Klick, A. Nowick, W. Sibley and E. Sonder, Point Defects in Solids, New York: Plenum Press, 1972.

[12] R. Heaton and C. Lin, "Electronic energy-band structure of the calcium fluoride crystal," *The American Physical Society,* vol. 22, no. 8, pp. 3629-3638, 1980.

[13] K. Schwartz, C. Trautmann, A. El-Said, R. Neumann, M. Toulemonde and W. Knolle, "Color-center creation in LiF under irradiation with swift heavy ions: Dependence on energy loss and fluence," *Physical Review B,* vol. 70, 2004.

[14] T. Ikeda, H. Kobayashi, Y. Ohmura, H. Nakamatsu and T. Mukoyama, "Electronic Structure of Alkaline-Earth Fluorides Studied by Model Clusters. I. Ground State," *JOurnal of the Physical Society of Japan,* vol. 66, no. 4, pp. 1074-1078, 1997.

[15] P. Feltham, "Colour Centres n Alkaline Earth Fluorides," *Physica status solidi,* vol. 10, no. 1, pp. 203-211, 1965.

[16] J. H. Hubbell and S. M. Seltzer, "X-Ray Mass Attenuation Coefficients," National Institute of Standards and Technology, 1993 [Online]. Available:

http://physics.nist.gov/PhysRefData/XrayMassCoef/ComTab/fluoride.html [Accessed 17 April 2017].

[17] International Atomic Energy AGency, "IAEA Photonuclear Data Library," October 2000 [Online]. Available: https://www-nds.iaea.org/photonuclear/ [Accessed 17 April 2017].

[18] "ASTM E2450-11 Standard Practice for Application of CaF2(Mn) Thermoluminescence Dosimeters in Mixed Neutron-Photon Environments," ASTM International, West Conshohocken, PA, 2011.

[19] D. Fitchen, W. Beall Fowler, C. Henry, M. Klein, R. Knox, F. Luty, H. Mahr, H. Seidel, C. Slichter, K. Teegarden and H. Wolf, Physics of Color Centers, London: Academic Press Inc. (London) Ltd, 1968.

[20] A. Gusarov, D. Doyle, A. Hermanne, F. Berghmans, M. Fruit, G. Ulbrich and M. Blondel, "Refractive-index changes caused by proton radiation in silicate optical glasses," *Applied Optics,* vol. 41, no. 4, pp. 678-684, 2002.

[21] S. Girard, J. Kuhnhenn, A. Gusarov, B. Brichard, M. Van Uffelen, Y. Ouerdane, A. Boukenter and C. Marcandella, "Radiation effects on silica-based optical fibers: Recent advamces and Future Challenges," *IEEE Transcations on Nuclear Science,* vol. 60, no. 3, pp. 2015-2036, 2013.

[22] H. Föll, "Iron, Steel and Swords," [Online]. Available: https://www.tf.uni-kiel.de/matwis/amat/iss/kap_5/backbone/r5_2_1.html [Accessed 5 May 2017].

[23] Y. Ma and M. Rohlfing, "Optical excitation of deep defect levels in insulators within many-body perturbation theory: The F center in calcium fluoride," *American Physical Society,* vol. 77, pp. 1-4, 2008.

[24] T. Basiev and S. Mirov, Room Temperature Tunable Color Center Lasers, Langhorne: Harwood Academic Publishers, 1994.

[25] G. Wertheim, A. Hausmann and W. Sander, The Electronic Structure of Point Defecta, Amsterdam: North-Holland Publishing Company, 1971.

[26] J. H. Beaumont, W. Hayes, G. P. Summers and J. W. Twidell, "Trapped hole centers in alkaline earth fluorides," *Solid State Communications,* vol. 6, pp. 903-906, 1968.

[27] A. Smakula, "Color centers in calcium fluoride and barium fluoride crystals," *Physical Review,* vol. 77, no. 3, pp. 408-409, 1950.

[28] A. Smakula, "Color Centers in Calcium Fluoride Crystals," Cambridge, 1954.

[29] H. Rabin and C. Klick, "Formation of F Centers at Low and Room Temperatures," *Physical Review,* vol. 117, no. 4, pp. 1005-1010, 1960.

[30] C. Catlow, "Radiation damage and photochromism in the alkaline earth fluorides," *Journal of Physical Chemistry,* vol. 12, pp. 969-988, 1979.

[31] T. Kamikawa and K. Ozawa, "Induced Color Centers in CaF2 Crystals Irradiated with Neutrons at Liquid Nitrogen Temperature," *Journal of the Physical Society of Japan,* vol. 24, no. 1, pp. 115-119, 1968.

[32] C. Flynn, Point defects and diffusion, Oxford: Clarendon Press, 1972.

[33] D. Messner and A. Smakula, "Color Centers in Alkaline Earth Fluorides," *Physical Review,* pp. 1162-1166, 1960.

[34] L. Su, J. Xu, W. Yang, X. Jiang, Z. Zhao, G. Zhou, H. Li and J. Si, "Effect of gamma irradiation on undoped and uranium doped calcium fluoride crystals," *Solid State Communication,* vol. 132, pp. 757-760, 2004.

[35] Shimadzu Corporation, *Instruction Manual, User's System Guide UV-1601 SHIMADZU RECORDING SPECTROPHOTOMETERS,* 1994.

[36] C. Wei, S. PingXin, D. YonhJun, Z. YingJiu and H. Wei, "Determination of color centers in CaF2 crystals by mutliple gamma-ray irradiations," *Chinese Science Bulletin,* vol. 58, no. 11, pp. 1321-1324, 2013.

[37] A. Smakula, "Color centers in Calcium Fluoride crystals," Document Service Center, Dayton, 1954.

[38] W. T. Silfvast, Laser Fundamentals, New York: Cambridge University Press, 2004.

APPENDIX

The nuclides present in the samples after being irradiated at the Oregon State University TRIGA reactor. Beyond Ca isotopes, this shows there are impurities present.

B15-3

Nuclide	HpGe Activity (μCi)
As-74	8.61E-02
Ca-47	5.47E-01
Eu-152	1.41E+00
Gd-153	5.14E-02
K-42	1.66E+00
La-140	4.45E-02
Na-24	5.75E-02
Sm-153	7.86E-01
Yb-175	3.18E-01

B15-5

Nuclide	HpGe Activity (μCi)
Ca-47	6.34E0
Eu-152	1.35E1
Sm-153	6.47E0
Ho-166	2.00E0
Na-24	4.96E-1
Eu-154	1.17E0
La-140	3.76E-1
Se-75	1.86E0
Nd-147	3.53E-1
As-74	3.58E-1
Gd-153	5.62E-1

B15-4

Nuclide	HpGe Activity (μCi)
Ca-47	1.99E1
Sm-153	16.327
Eu-152	11.528
Eu-154	2.6824
Na-24	7.35E-1
La-140	.98039
Np-239	.57227
Yb-175	1.1093
Se-75	2.5054
As-74	.6753
Ba-131	.81427
Gd-153	1.1244
Sr-85	.18964
Co-58	.079456